

Extreme matter in electromagnetic fields and rotation

Kenji Fukushima

Department of Physics, The University of Tokyo, 7-3-1 Hongo, Bunkyo-ku, Tokyo 113-0033, Japan

July 21, 2022

Abstract

We look over recent developments on our understanding about relativistic matter under external electromagnetic fields and mechanical rotation. I review various calculational approaches for concrete physics problems, putting my special emphasis on generality of the method and the consequence, rather than going into phenomenological applications in a specific field of physics. The topics covered in this article include static problems with magnetic fields, dynamical problems with electromagnetic fields, and phenomena induced by rotation.

Contents

1	Introduction	2
2	Static Problems with Magnetic Fields	5
2.1	Calculus with constant magnetic field	5
2.1.1	Solutions of the Dirac equation	5
2.1.2	Schwinger proper-time method	7
2.2	Magnetic Catalysis	8
2.2.1	Direct calculation	10
2.2.2	Renormalization group analysis	11
2.3	Inverse Magnetic Catalysis	13
2.3.1	Finite density	13
2.3.2	Finite temperature	14
2.4	Toward more realistic descriptions	15
2.4.1	Solvable example of inhomogeneous magnetic field	15
2.4.2	Finite size and surface effect	16
3	Dynamical Problems with Electromagnetic Fields	19
3.1	Schwinger Mechanism	19
3.1.1	Solvable example of time-dependent electric fields	20
3.1.2	Worldline instanton approximation	22
3.2	Chiral Anomaly and Axial Ward Identity	25
3.2.1	In- and out-states	26
3.2.2	Optical realization of the chiral magnetic effect	28

4	Phenomena induced by Rotation	30
4.1	Rotating Chiral Fermions	31
4.1.1	Field-theoretical treatments	31
4.1.2	Chiral vortical effect	32
4.2	Floquet Theory	33
4.2.1	Rotating frame and Magnus expansion	34
4.2.2	Interpretation as an artificial electric field	35
4.3	Relativistic Gyromagnetic Effects	36
4.3.1	Chiral Barnett effect	36
4.3.2	Chiral Einstein-de Haas effect	37
5	Summary	38

1 Introduction

This review is not intended to be a comprehensive chapter of encyclopedia but a collection of selected topics on relativistic matter (i.e., matter with fermions having relativistic energy dispersion relations) affected by external electromagnetic fields and/or rotation, which may have applications in various physics contexts. In this review, however, I would not go into applications but will put my emphasis on methodologies, assuming that readers are already engaged in some physics problems with electromagnetic fields and/or rotation, and are rather interested in practical approaches. If one is interested in applications in condensed matter physics, one is invited to read Refs. [1, 2]. In the context of the high-energy nuclear reactions, Ref. [3] provides us with the state-of-the-art phenomenological progresses among which the topologically induced effects are nicely summarized previously in Ref. [4].

In the present review this introduction will be followed by three sections focused on three different but related topics. In the next section we will explicitly see instructive and convenient calculus to deal with external magnetic field \mathbf{B} . The most remarkable and universal feature of relativistic matter is the magnetic catalysis induced by constant \mathbf{B} , on which this present review cannot avoid having some overlap with other articles, see, e.g., Ref. [2]. In this review we will elucidate, on top of direct calculation, the renormalization group argument to deepen our intuitive understanding on the magnetic catalysis.

Furthermore, in addition to the well-known (inverse) magnetic catalysis, we will address two important but technically involved topics to upgrade postulated setups to more realistic situations. One is the effect of inhomogeneous $\mathbf{B}(\mathbf{x})$ and the other is the effect of boundary imposed for finite size systems. These are, definitely, distinct effects, but they have similarity to some extent, leading to modifications on the Landau levels.

For inhomogeneity, fortunately, a special profile of the magnetic field is known, for which the Dirac equation can be analytically solved. This special case is often referred to as the Sauter-type potential problem. We will see a similar Sauter-type problem when we discuss electric fields later. Thanks to this solvable example, we can acquire some useful insights about how spatial inhomogeneity should modify the conventional pattern of the Landau degeneracy. Such rigorous results are valid only for a specific example of $\mathbf{B}(\mathbf{x})$, but we may well expect to learn general qualitative features related to inhomogeneous $\mathbf{B}(\mathbf{x})$. The Landau degeneracy would be lifted up also by a different physical disturbance, that is, the finite size effect even for homogeneous magnetic fields. We will show explicit calculations with a boundary in the cylindrical coordinates. We will go into rather technical details here; some of the expressions will be useful in later discussions on rotation.

Here, in this review, we would not consider time-dependent $\mathbf{B}(t)$. For static magnetic fields we can utilize time-independent vector potentials, and the ground state of matter under such static magnetic

fields may stably exist. It is a theoretically intriguing problem to identify the ground state structures as functions of static magnetic strength. Then, naturally, one may think that a time-dependent $\mathbf{B}(t)$ should be far more challenging and interesting enough to deserve closer discussions. In fact, however, there are (at least) two reasons for our sticking to static magnetic fields. The first and crucial reason is that a nonperturbative analysis with time-dependent $\mathbf{B}(t)$ is impossibly difficult, while a diagrammatic method may work perturbatively if \mathbf{B} is sufficiently weak or $\mathbf{B}(t)$ behaves like a sharp pulse to justify the impulse approximation. There is no Sauter-type solvable problem known for time-dependent $\mathbf{B}(t)$. One might wonder if one can anyway solve the Dirac equation numerically instead of pursuing an analytical solution, but such an even brute-force calculation would suffer principle difficulty. Numerical calculations inevitably rely on lattice discretization and a certain scheme of boundary condition. The possible magnetic flux is quantized in order to satisfy imposed boundary condition. Therefore, continuously changing $\mathbf{B}(t)$ as a function of time would be impossible in such lattice discretized systems. The second reason for our focusing on time-independent \mathbf{B} in this review is that we would like to address the effect of electric field \mathbf{E} mainly from the dynamical point of view. The difference between \mathbf{B} and \mathbf{E} appears from quantum numbers of these fields; \mathbf{B} is \mathcal{T} -odd and \mathcal{P} -even, and \mathbf{E} is \mathcal{T} -even and \mathcal{P} -odd. This means that the time-derivative, $\dot{\mathbf{B}}$, is \mathcal{T} -even as is \mathbf{E} , resulting in similar dynamical evolutions, though they are opposite in the parity. So, if we place an electrically charged particle into a system under either $\dot{\mathbf{B}}$ or \mathbf{E} , the field gives a finite energy to the particles and accelerates them. More interestingly, if the given energy exceeds a mass threshold, a pair of an onshell particle and an onshell anti-particle is created, which is called the Schwinger Mechanism.

The next section after static magnetic field is devoted to discussions on the Schwinger Mechanism for spatially homogeneous electric field. For a comprehensive review on the Schwinger Mechanisms and the effective Lagrangians, see Ref. [5]. If electromagnetic fields themselves are time-dependent, the pair production of a particle and an anti-particle is simply an inverse process of the annihilation. What is particularly remarkable about the Schwinger Mechanism is that even a static \mathbf{E} is intrinsically dynamical, while a static \mathbf{B} cannot transfer any work onto charged particles. To concentrate on effects solely induced by \mathbf{E} , as we mentioned above, we will limit ourselves to the case with time-independent \mathbf{B} throughout this review.

There are many formulations and derivations for the particle production rate associated with the Schwinger Mechanism. In this review I will present somehow explicit calculations using the Sauter-type potential for time-dependent $\mathbf{E}(t)$, which also includes static \mathbf{E} as a special limit. In principle, the strategy to derive the pair production rate can be generalized to arbitrary electromagnetic backgrounds with help of some numerical calculations. Although there are tremendous progresses in the numerical techniques (for such an example, see Ref. [6]), we will pursue only the analytical approaches in this review. For this purpose I will give detailed explanations on a saddle-point approximation within the framework of the worldline formalism. The worldline formalism is based on Schwinger's proper-time integration. Interestingly, in the saddle-point approximation, the sum over multi-particle production corresponds to the sum over the winding number which classifies classical solutions of the equation of motion. Thus, the calculational machinery employed with the saddle-point approximation is commonly referred to as the "worldline instanton" approximation.

The presence of both \mathbf{E} and \mathbf{B} with $\mathbf{E} \cdot \mathbf{B} \neq 0$ provides us with the simplest optical setup to probe a non-trivial sector with respect to the chiral anomaly. When the fermion mass m is vanishing, the axial vector current is expected to be conserved, but quantum fluctuations give rise to a violation of the would-be current conservation. That is, the divergence of the axial vector current is no longer zero but is proportional to $\mathbf{E} \cdot \mathbf{B}$ if there are those background fields. We shall pay our attention to the chiral anomaly using the proper-time integration, to notice that taking the $m \rightarrow 0$ limit turns out to be a subtle procedure. With concrete calculations we will demonstrate the importance to distinguish the in-state and the out-state once the system involves background \mathbf{E} ; the expectation values of physical observables are calculable with the in-in expectation values, while the in-out expectation values are

amplitudes whose squared quantities correspond to the expectation values of physical observables. As an application of the in- and out-state calculus we will cover an optical realization of the chiral anomaly. One clear signature for the chiral anomaly is an anomalous contribution to the electric resistance called the negative magnetoresistance. The microscopic picture can be established as a manifestation of the chiral magnetic effect (CME) (which is one of central subjects of Ref. [4]; see also Ref. [7] for a memorial essay on the CME).

Finally, we shall turn to discussions on effects induced by mechanical rotation. There are two possibly equivalent but technically very different approaches to deal with rotation; one is the field-theoretical calculation in a rotating frame, for which the rotation is global, and the other is the fluid dynamical description with vorticity vectors, for which the rotation is local. If the local vorticity vector uniformly distributes over two-dimensional space, it eventually amounts to the rigid rotation, as is the case for the vortex lattice of a rotating superfluid (see, for example, Ref. [8]). Therefore, these two treatments should be in principle equivalent, and nevertheless, each method has some advantages and disadvantages. The advantage to use the local vorticity vector is that only the local properties are concerned and it is not necessary to impose a boundary not to break the causality. However, the price to pay is, one must know a correct theoretical reduction to fluid dynamics in such a way to keep essential features of the chiral anomaly. Such a reduction program is, to some extent, successful, leading to the chiral kinetic theory and the anomalous hydrodynamics.

Solving the Dirac equation in a rotating frame is a rather brute-force method, but the advantage is that one does not have to worry about a theoretical reduction to slow variables. Once the solutions of the Dirac equation are given, all necessary information must be contained in those solutions. In this review I take my preference to proceed into technical details on the field-theoretical treatments in a rotating frame. In this way we will see a derivation of the chiral vortical effect (CVE), which is an analogue of the CME with the magnetic field replaced by the rotation (see Ref. [4] for more details). Such an explicit calculation will give us a useful insight into the microscopic origin of the CVE – unlike the quantum anomaly which typically originates from the ultraviolet edges of the momentum integration, the CVE emerges from a finite discrepancy between a continuous integral and a discrete sum, which is rather analogous to the Casimir effect on the technical level.

Another interesting feature of rotating system is found in the application of the Floquet theory which states a mathematical theorem on differential equations with periodic dependence (see, e.g., Refs. [9, 10] for pedagogical reviews). We can regard electromagnetic fields in a rotating frame as time periodically driven forces, and several techniques are known to tackle such Floquet-type problems. It is impossible to cover the whole stories about the Floquet theory, and so we will take a quick view of a technology called the Magnus expansion, which is a common method to make the Floquet problem well-defined from the high-frequency rotation limit. Also, we point out that the Floquet theory has a fascinating interpretation as a higher (spatial) dimensional theory with an external electric field whose strength is related to the frequency. I will explain this interesting correspondence from a motivation that our knowledge on dynamical problems with electromagnetic fields could have an interdisciplinary application to consider the Floquet-type problem. In other words, instead of imposing an external electric field, one may think of shaking a system time periodically to mimic the effect of electric field. This idea might remind us of the synthetic magnetic field realized by the Floquet engineering (see Ref. [11] for a review) but the interpretation of electric field is rather simpler.

The last topics discussed in this review are relativistic extensions of the gyromagnetic effects, namely, the Barnett effect and the Einstein-de Haas effect (for an established and the most comprehensive review, see Ref. [12]). It is a widely known notion that the mechanical rotation and the magnetization can be converted to each other; precisely speaking, the orbital angular momentum can be converted to the spin due to the spin-orbit coupling, and vice versa. This conversion itself is a quite robust process, which implies that the relativistic extensions be straightforward. In relativistic theories, however, the separation of the total angular momentum into the orbital and the spin components is ambiguous. It

is thus still under disputes whether the relativistic Barnett and Einstein-de Haas effects can exist as straightforward generalization of classical descriptions. I will introduce some interesting theoretical speculations, hoping that this part of the present review will be followed up by future research.

Before closing the introduction, let us make sure conventions assumed for the present review. Throughout this review, we consistently use words, “static”, “homogeneous”, and “constant” in the following way. Static \mathbf{E} and \mathbf{B} mean time-independent fields, i.e., $\dot{\mathbf{E}} = 0$ and $\dot{\mathbf{B}} = 0$. Homogeneous fields are independence of spatial coordinates, that is, $\partial_x \mathbf{E} = 0$ and $\partial_x \mathbf{B} = 0$ where x is any of spatial coordinates. For static and homogeneous electromagnetic fields, we often call them constant. In Minkowskian spacetime our choice of coordinates is (x^0, x^1, x^2, x^3) and $x_0 = x^0$, $x_1 = -x^1$, $x_2 = -x^2$, $x_3 = -x^3$. We often use x , y , z to denote x^1 , x^2 , x^3 . For momenta we employ similar conventions and p_x , p_y , p_z often indicate p^1 , p^2 , p^3 . This rule is applied also for \mathbf{E} and \mathbf{B} . In Euclidean spacetime (x^4, x^1, x^2, x^3) and (x_4, x_1, x_2, x_3) are just indistinguishable.

Finally, we note that $\hbar = c = 1$ and $\varepsilon_0 = \mu_0 = 1$ in the natural unit. Moreover, in this review, we will not treat the in-medium electromagnetic fields, so we will thoroughly employ the electric field \mathbf{E} and the magnetic flux \mathbf{B} , but never use the electric flux \mathbf{D} nor the magnetic strength \mathbf{H} in this review. (There is no difference for the vacuum fields in the natural unit.)

2 Static Problems with Magnetic Fields

The Maxwell equations have duality between the electric field \mathbf{E} and the magnetic field \mathbf{B} , which is often referred to as Heaviside-Larmor symmetry. Since the temporal and the spatial directions are not equivalent in Minkowskian spacetime, however, there is a tremendous difference in effects of \mathbf{E} and \mathbf{B} upon matter. In most of our considerations in the present review we limit ourselves to static \mathbf{E} and \mathbf{B} . One might then think of static problems of matter under such static \mathbf{E} and \mathbf{B} ; however, a static \mathbf{E} would induce an electric current (if matter is not an insulator), and strictly speaking, such a system with a sustained current can never be equilibrated but it is a steady state. In contrast, a static \mathbf{B} would not transfer any work on charged particles, and one can consider an equilibrated system even at finite but static \mathbf{B} , which is our main subject of this section.

2.1 Calculus with constant magnetic field

It is a textbook knowledge how to solve the Schrödinger equation in constant \mathbf{B} to derive the Landau quantization. There is, however, almost no textbook that explains how to solve the Dirac equation with constant \mathbf{B} . Some complication appears from the fact that the Dirac spinors have components with different spin polarizations which respond to \mathbf{B} differently. In this subsection we make a quick summary of the most naive calculations of solving the Dirac equation in detail. As we will see in the next subsection, for practical purposes, an alternative formulation based on the proper-time integration turns out much more convenient. Nevertheless, explicit calculations are quite instructive, as explicated in this subsection.

2.1.1 Solutions of the Dirac equation

We here review a direct method to solve the Dirac equation as a straightforward extension from the standard technique for the Schrödinger equation. In the literature this method is often called the Ritus method [13]. We can fix the direction of \mathbf{B} along the z -axis without loss of generality, and shall choose a gauge, $A^0 = A^1 = A^3 = 0$ and $A^2 = Bx$, corresponding to $\mathbf{B} = \nabla \times \mathbf{A} = B\hat{\mathbf{e}}_z$. In the following we always assume $eB > 0$ to avoid putting modulus and simplify the expressions. Then, let us introduce

two functions using the harmonic oscillator wave-functions:

$$\begin{aligned} f_{n,p}^+(x) &\equiv e^{-i(\omega t - p_y y - p_z z)} \phi_n(x - p_y/eB) \quad (n = 0, 1, \dots) \\ f_{n,p}^-(x) &\equiv e^{-i(\omega t - p_y y - p_z z)} \phi_{n-1}(x - p_y/eB) \quad (n = 1, 2, \dots) \end{aligned} \quad (1)$$

and $f_{0,p}^-(x) = 0$. For the harmonic oscillator wave-functions the frequency is characterized by the magnetic scale as

$$\phi_n(x) \equiv \sqrt{\frac{1}{2^n n!}} \left(\frac{eB}{\pi}\right)^{1/4} e^{-\frac{1}{2}eBx^2} H_n(\sqrt{eB}x), \quad (2)$$

where $H_n(x)$ represents the Hermite polynomials of degree n . Now, let us introduce a 4×4 projection matrix as

$$P_{n,p}(x) \equiv \frac{1}{2} [f_{n,p}^+(x) + f_{n,p}^-(x)] + \frac{i}{2} [f_{n,p}^+(x) - f_{n,p}^-(x)] \gamma^1 \gamma^2, \quad (3)$$

which is reduced to $P_{n=0,p}(x) = P_+$ for the lowest Landau level with $P_{\pm} = \frac{1}{2}(1 \pm i\gamma^1 \gamma^2)$. After several line calculations one can easily find the following relation,

$$(i\cancel{\partial} - e\cancel{A} - m)P_{n,p}(x) = P_{n,p}(x)(\omega\gamma^0 + \sqrt{2eBn}\gamma^2 - p_z\gamma^3 - m). \quad (4)$$

At this point, using the above relation, we can readily write down the solutions of the Dirac equation. Changing the order of the Dirac operator and the projection operator makes the right-hand side be a form of the free Dirac equation with the momenta replaced as $p \rightarrow \tilde{p} = (\omega, 0, -\sqrt{2eBn}, p_z)$. Thus, the solutions of the Dirac equation at finite constant \mathbf{B} read,

$$\psi(n, p; x) = P_{n,p}(x) u(\tilde{p}, s), \quad \psi(n, p; x) = P_{n,p}(x)^* v(\tilde{p}, s) \quad (5)$$

for particles and anti-particles. Here, the explicit expressions for spinors in momentum space are,

$$u(\tilde{p}, s) = \frac{1}{\sqrt{\omega + m}} \begin{pmatrix} (\omega + m)\xi_s \\ \boldsymbol{\sigma} \cdot \tilde{\mathbf{p}} \xi_s \end{pmatrix}, \quad v(\tilde{p}, s) = \frac{1}{\sqrt{\omega + m}} \begin{pmatrix} \boldsymbol{\sigma} \cdot \tilde{\mathbf{p}} \eta_s \\ (\omega + m)\eta_s \end{pmatrix} \quad (6)$$

in the Dirac representation of the γ matrices. For perturbative calculations the free propagator is the most elementary building block of Feynman diagrams, which can be immediately constructed with the solutions of the Dirac equation. The propagator then has such an explicit form of the momentum integration and the Landau level sum as

$$S_0^F(x, y) = \langle T\psi(x)\bar{\psi}(y) \rangle = \int \frac{d\omega dp_y dp_z}{(2\pi)^3} \sum_n P_{n,p}(x) \frac{i(\cancel{\not{p}} + m)}{p_{\parallel}^2 - 2eBn - m^2 + i\epsilon} P_{n,p}^*(y). \quad (7)$$

Here, $p_{\parallel} \equiv (\omega, 0, 0, p_z)$. It is important to make several remarks here about the above propagator. Sometimes I see a bit misleading statement about \tilde{p} as if \tilde{p} were a genuine momentum flowing on a fermionic propagator, but such a naive picture would violate the momentum conservation at vertices of the Yukawa coupling. I would make a next comment about the translational invariance. For constant \mathbf{B} the system should keep the translational invariance, which implies that $S_0^F(x, y)$ be a function of $x - y$ alone, but the vector potential \mathbf{A} is x dependent and it seemingly violates the translational invariance. In fact, obviously, $S_0^F(x, y)$ is not a function of $x - y$, but as we will confirm soon later, it is only a phase that breaks the translational invariance.

We note that the propagator in the lowest Landau level approximation (LLLA) obtains from $n = 0$, that is,

$$\begin{aligned} S_{\text{LLLA}}^F(x, y) &= \int \frac{d\omega dp_y dp_z}{(2\pi)^3} e^{-i\omega(x^0 - y^0) + ip_y(x^2 - y^2) + ip_z(x^3 - y^3)} \\ &\quad \times \sqrt{\frac{eB}{\pi}} e^{-\frac{1}{2}eB[(x^1 - p_y/eB)^2 + (y^1 - p_y/eB)^2]} \frac{i(\cancel{\not{p}}_{\parallel} + m)P_+}{p_{\parallel}^2 - m^2 + i\epsilon}. \end{aligned} \quad (8)$$

From this form it is obvious again that $S_{\text{LLLA}}^F(x, y)$ is not a function of $x - y$. Interestingly, we can easily separate the translational invariant and the non-invariant parts after the p_y integration, leading to the following expression,

$$S_{\text{LLLA}}^F(x, y) = e^{i\frac{eB}{2}(x^1+y^1)(x^2-y^2)} \cdot \frac{eB}{2\pi} e^{-\frac{eB}{4}[(x^1-y^1)^2+(x^2-y^2)^2]} \times \int \frac{d\omega dp_z}{(2\pi)^2} e^{-i\omega(x^0-y^0)+ip_z(x^3-y^3)} \frac{i(\not{p}_{\parallel} + m)P_+}{p_{\parallel}^2 - m^2 + i\epsilon}. \quad (9)$$

This overall phase factor is nothing but the Aharonov-Bohm (AB) phase by $\exp(-ie \int_y^x dz_{\mu} A^{\mu})$ with the vector potential representing \mathbf{B} . For most loop calculations the phase factors cancel out, and it is convenient to introduce the Fourier transformation of the phase removed part, $\tilde{S}(x-y) = e^{ie \int_y^x dz_{\mu} A^{\mu}} S(x, y)$. The translational invariant part of the LLLA propagator in momentum space thus reads,

$$\tilde{S}_{\text{LLLA}}^F(p) = \frac{i(\not{p}_{\parallel} + m)P_+ 2e^{-p_{\perp}^2/eB}}{p_{\parallel}^2 - m^2 + i\epsilon}, \quad (10)$$

where $p_{\perp}^2 \equiv p_x^2 + p_y^2$. The last exponential damping factor is important; the well-known Landau degeneracy factor, $eB/(2\pi)$, appears from the integrations over p_x and p_y which are convergent thanks to this exponential damping factor.

Indeed, it is important to note that the transverse momentum dependence appears only through $e^{-p_{\perp}^2/eB}$, so that the integration over transverse phase space is separately performed, leading to the Landau degeneracy factor,

$$\int \frac{d^2 p_{\perp}}{(2\pi)^2} 2e^{-p_{\perp}^2/eB} = \frac{eB}{2\pi}. \quad (11)$$

Now that the transverse integration is done, the (3+1)-dimensional dynamics is subject to restricted space along the t - and z -axes, that is, the system is effectively reduced to (1+1) dimensions. We must emphasize that the particle motion in configuration space is not restricted at all, but there is no energy cost with transverse motions, which results in the dimensional reduction. A short summary on the LLLA is:

LLLA: The energy integrands have only trivial dependence on the transverse momenta, p_{\perp}^2 , and the transverse phase space leads to the Landau degeneracy factor, $eB/(2\pi)$. The rest of the phase space integration is reduced to (1+1) dimensions along the t - and z -axes.

Apart from whether it is a good approximation or not, the LLLA is quite useful for us to understand the magnetic effect qualitatively.

2.1.2 Schwinger proper-time method

Next, let us see how to find the same expression from a completely different passage which is much shorter than solving the Dirac equation directly.

Schwinger developed a useful method [14] for general electromagnetic backgrounds. The idea is that, if we are interested in the propagator only, we do not have to solve the Dirac equation but what we should do is just to take an inverse of the Dirac operator with the electromagnetic fields contained in the covariant derivative. Another important step for the actual calculation is that the operator inverse can be expressed in an integral form with inclusion of an auxiliary variable, s , which is called the proper time. That is, with a notation of D_{μ} for the covariant derivative, we can write,

$$S_0^F(x, y) = \langle x | \frac{i(\not{D} + m)}{-\not{D}^2 - m^2 + i\epsilon} | y \rangle = (i\not{D}_x + m) \int_0^{\infty} ds \langle x | \exp[i(-\not{D}^2 - m^2 + i\epsilon)s] | y \rangle. \quad (12)$$

We note that \not{D}^2 produces a matrix, $\exp(-\frac{i}{2}eF \cdot \sigma s)$ with $F \cdot \sigma = F_{\mu\nu}\sigma^{\mu\nu}$, where the spin tensor is defined as usual; $\sigma^{\mu\nu} \equiv \frac{i}{2}[\gamma^\mu, \gamma^\nu]$. Then, it is an easy exercise to find,

$$e^{-\frac{i}{2}eF \cdot \sigma s} = \cos(eBs) [1 + \gamma^1 \gamma^2 \tan(eBs)]. \quad (13)$$

In this way we can continue sorting out the expression, and after all, we can extract $\tilde{S}_0^F(x-y)$, which can be Fourier transformed into $\tilde{S}_0^F(p)$ given by [14, 15, 16],

$$\begin{aligned} \tilde{S}_0^F(p) = \int_0^\infty ds \exp \left[-i \left(m^2 + \omega^2 + p_z^2 + p_\perp^2 \frac{\tan(eBs)}{eBs} \right) s \right] \\ \times [\not{p} + m + (p_y \gamma^1 - p_x \gamma^2) \tan(eBs)] \cdot [1 + \gamma^1 \gamma^2 \tan(eBs)]. \end{aligned} \quad (14)$$

This expression for the propagator is so useful that we will later revisit this including the electric field when we discuss the worldline instanton approximation and also the axial Ward identity. It is not easy, however, to implement the LLLA from the above expression. Interestingly, it is possible to reexpress the above propagator into the following form [16, 17],

$$\tilde{S}^F(p) = \sum_{n=0}^\infty \frac{i \{ (\not{p}_\parallel + m) [P_+ A_n(p_\perp^2) + P_- A_{n-1}(p_\perp^2)] + \not{p}_\perp B_n(p_\perp^2) \}}{p_\parallel^2 - 2eBn - m^2 + i\epsilon}, \quad (15)$$

where the sum over n corresponds to the Landau level sum. The numerator consists of two functions, $A_n(p_\perp^2) \equiv 2e^{-2z}(-1)^n L_n^{(0)}(4z)$ and $B_n(p_\perp^2) \equiv 4e^{-2z}(-1)^n L_{n-1}^{(1)}(4z)$ with $z \equiv p_\perp^2/(2eB)$. Here, $L_n^{(\alpha)}(x)$ denotes the generalized Laguerre polynomials defined by

$$L_n^{(\alpha)}(x) \equiv \frac{e^x x^{-\alpha}}{n!} \frac{d^n}{dx^n} (e^{-x} x^{n+\alpha}). \quad (16)$$

From this expanded form, we can deduce the LLLA propagator immediately from $n=0$, which exactly reproduces Eq. (10). Usually, if eB is large enough as compared to other energy scales in the problem, the LLLA works excellently to capture the essence.

2.2 Magnetic Catalysis

Now we are ready to understand what the magnetic catalysis is, which is a phenomenon of abnormal enhancement of a scalar condensate. We can write the scalar condensate in terms of the propagator as

$$\Sigma = \langle \bar{\psi} \psi \rangle = - \lim_{y \rightarrow x} \text{tr} S(x, y) = - \lim_{z \rightarrow 0} \text{tr} \tilde{S}(z). \quad (17)$$

This quantity measures a condensate formed with a particle and an anti-particle (or a hole at finite density) and is generally induced if the interaction is strong enough. From the physics point of view, $\bar{\psi} \psi$ is an operator conjugate to the mass, since the mass term in the Dirac Lagrangian density is $m \bar{\psi} \psi$, which means that $\Sigma \neq 0$ would play a role as a source term to induce a larger effective mass. In this section we will quantify the relation between the bare masses and the effective masses in the presence of the scalar condensate.

Condensates or the vacuum expectation values of physical operators should generally depend on external parameters such as the temperature, the density, and the electromagnetic background fields. It is thus an interesting question how Σ changes when a finite \mathbf{B} is turned on as studied in a pioneering work of Ref. [18]. Intuitively, it is naturally anticipated that \mathbf{B} would favor a formation of the scalar condensate from the following argument. To assign proper quantum numbers to a composite state of a particle and an anti-particle, in the non-relativistic language, the scalar condensate must have the

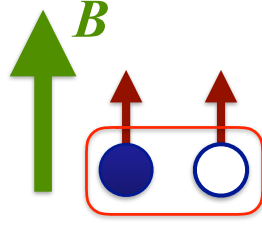


Figure 1: Schematic illustration for magnetic enhancement of the scalar condensate.

orbital angular momentum $L = 1$ to cancel the intrinsic parity which is opposite for a particle and an anti-particle. Then, $S = 1$ is required to make the total angular momentum $J = 0$. Even though the whole quantity, $\bar{\psi}\psi$, is charge neutral and has no direct coupling to \mathbf{B} , from the microscopic level, we may well expect that such a spin-triplet configuration could be intrinsically more favored by \mathbf{B} , which is schematically illustrated in Fig. 1.

In most interested cases, $\Sigma(B)$, i.e., the scalar condensate as a function of magnetic strength $B = |\mathbf{B}|$ should increase with increasing B . Such increasing behavior is actually the case in the strong interaction physics in which the low-energy theorem holds including the magnetic effect [19], which is revisited more extensively in Ref. [20]. Although this tendency itself is rather robust not sensitive to specific theory, the precise dependence on B should be different for different interactions and degrees of freedom contained in the theory. In the literature, this general tendency of increasing Σ with increasing magnetic strength B is referred to as the magnetic catalysis.

In the original context [16, 21], however, the magnetic catalysis is defined in a more strict manner. It has been found that the magnetic field plays a role as a catalyst to cause nonzero Σ for even infinitesimal coupling λ . The statement shall be:

Magnetic Catalysis: The scalar condensate takes a nonzero expectation value for even infinitesimal attractive coupling if the system is placed under sufficiently strong magnetic field.

Roughly speaking, the system under strong magnetic fields is effectively reduced to (1+1) dimensions. Then, the gap equation for Σ exhibits the same structure as that for the gap energy in superconductivity, for which high density realizes one dimensionality on the Fermi surface. In fact, plugging Eq. (14) into Eq. (17), performing the four-momentum integration which yields eBs^{-1} to compensate for the mass dimension 4, we finally get,

$$\Sigma \simeq -\frac{eB}{4\pi^2}m \int_{1/\Lambda^2}^{\infty} ds s^{-1} e^{-im^2s} \cot(eBs) \simeq -\frac{eB}{4\pi^2}m\Gamma[0, m^2/\Lambda^2], \quad (18)$$

where a ultraviolet cutoff Λ is adopted and $\Gamma[a, x]$ denotes the incomplete gamma function. To arrive at the last expression, the integration contour is rotated as $is \rightarrow s$ and then $\coth(eBs)$ is approximated to be unity for large eB , which corresponds to the LLLA. Because $\Gamma[0, x] \sim -\gamma_E - \ln x$ for small x , we understand that Σ should behave like $\sim m \ln m$ for small m . The operator $\bar{\psi}\psi$ is conjugate to m , so that Σ is obtained by the m -derivative of the energy $E[m]$. Therefore, such behavior of $\Sigma \sim m \ln m$ means that $E[m]$ should contain a term $\sim m^2 \ln m$. This observation will be soon verified in the subsection where we will see a model calculation of Σ as a function of B and the coupling λ .

2.2.1 Direct calculation

My goal in this subsection is to present direct calculations employing an interacting model. The model is defined with the following Lagrangian density:

$$\mathcal{L} = \bar{\psi} i \not{\partial} \psi + \frac{\lambda_\Lambda}{2} [(\bar{\psi} \psi)^2 + (\bar{\psi} i \gamma_5 \boldsymbol{\tau} \psi)^2], \quad (19)$$

for which the bare mass is assumed to be vanishing, $m = 0$, and λ_Λ is the coupling at the ultraviolet scale Λ . This type of model is commonly called the Nambu–Jona-Lasinio (NJL) model (for extensive reviews on the NJL model, see Refs. [22, 23]), which is a relativistic extension of the BCS model.

In the mean-field approximation, a quantum field is decomposed as $\bar{\psi} \psi = (\bar{\psi} \psi - \langle \bar{\psi} \psi \rangle) + \langle \bar{\psi} \psi \rangle$, with which higher-order fluctuations in $\bar{\psi} \psi - \langle \bar{\psi} \psi \rangle$ are neglected. In this approximation the mean-field Lagrangian density reads:

$$\mathcal{L}_{\text{MF}} = \bar{\psi} i \not{\partial} \psi + \lambda_\Lambda \langle \bar{\psi} \psi \rangle - \frac{\lambda_\Lambda}{2} \langle \bar{\psi} \psi \rangle^2 = \bar{\psi} (i \not{\partial} - M) \psi - \frac{M^2}{2\lambda_\Lambda}. \quad (20)$$

Now we understand that $\langle \bar{\psi} \psi \rangle$ gives rise to an effective mass term, namely, $M = -\lambda_\Lambda \langle \bar{\psi} \psi \rangle$. To determine the energetically favored value of M , we need to evaluate the energy E as a function of M , that is given in the mean-field approximation by

$$E[M] = -2 \int_{p^2 \leq \Lambda^2} \frac{d^3 p}{(2\pi)^3} \sqrt{p^2 + M^2} + \frac{M^2}{2\lambda_\Lambda}, \quad (21)$$

where Λ is the ultraviolet cutoff scale. The first term represents the zero-point oscillation energy, and the second is the condensation energy from the mean field. Introducing a dimensionless variable, $\xi \equiv M/\Lambda$, the energy can be expanded as

$$E[\xi] \simeq -\frac{\Lambda^4}{4\pi^2} (1 + \xi^2) + \frac{\Lambda^2}{2\lambda_\Lambda} \xi^2 + O(\xi^4). \quad (22)$$

The trivial vacuum at $\xi = 0$ becomes unstable when the quadratic coefficient in front of ξ^2 is negative. There are two competing effects for this coefficient; the zero-point oscillation energy always has a negative coefficient favoring a nonzero ξ , while the condensation contribution has the opposite sign. Therefore, if the coupling λ_Λ is large enough, the condensation energy is suppressed, and the zero-point oscillation energy overcomes to lead to a finite ξ or M . Thus, the spontaneous generation of dynamical mass $M \neq 0$ requires a large enough λ_Λ , i.e.,

$$\lambda_\Lambda \Lambda^2 > 2\pi^2. \quad (23)$$

We need higher-order terms $\sim O(\xi^4)$ to locate an optimal value of ξ .

Let us repeat the same procedure for the system with strong magnetic field. For simplicity the magnetic field is assumed to be strong enough to justify the LLLA in which the phase space integration is replaced by the Landau degeneracy factor and the (1+1)-dimensional integration:

$$2 \int_{p^2 \leq \Lambda^2} \frac{d^3 p}{(2\pi)^3} \longrightarrow \frac{eB}{2\pi} \int_{p^2 \leq \Lambda^2} \frac{dp_z}{2\pi}. \quad (24)$$

We note that there is only one spin degrees of freedom in the LLLA as a result of the projection by P_+ , and so the overall spin factor 2 does not appear in the right-hand side in the LLLA above. Then, we can compute the energy as

$$E[M] = -\frac{eB}{2\pi} \int_{-\Lambda}^{\Lambda} \frac{dp_z}{2\pi} \sqrt{p_z^2 + M^2} + \frac{M^2}{2\lambda_\Lambda} \simeq -\frac{eB\Lambda^2}{4\pi^2} \left[1 + \left(\ln \frac{2}{\xi} + \frac{1}{2} \right) \xi^2 \right] + \frac{\Lambda^2}{2\lambda_\Lambda} \xi^2 + O(\xi^4). \quad (25)$$

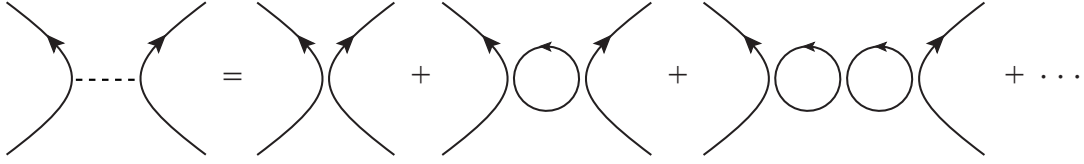


Figure 2: RG resummation diagrams for the four fermionic vertex.

This form of the expanded energy is extremely interesting. As we promised, a term $\sim M^2 \ln M$ appears. Thus, the quadratic coefficient is M or ξ dependent, and for $\xi \ll 1$, the coefficient involving $\ln(2/\xi)$ becomes arbitrarily large, which means that the negative coefficient can always overcome to make $\xi \rightarrow 0$ unstable for even infinitesimal coupling λ_Λ . Therefore, some $\xi \neq 0$ is energetically favored as long as eB and λ_Λ are non-vanishing, and the condition (23) in this case is changed to $\lambda_\Lambda > 0$. From the above expression of $E[M]$, surprisingly, we can find an energy minimum even without $O(\xi^4)$ term. Some calculations eventually concludes,

$$M_0 = \xi_0 \Lambda = 2\Lambda \exp\left(-\frac{2\pi^2}{\lambda_\Lambda eB}\right). \quad (26)$$

The analogy to superconductivity is evident in view of the above expression. The λ_Λ dependence enters the gap as an essential singularity around $\lambda_\Lambda = 0$, which is common to the BCS gap energy.

2.2.2 Renormalization group analysis

It would be quite instructive to consider an alternative approach to understand the magnetic catalysis based on the renormalization group (RG) equation following discussions in Refs. [24, 25]. This RG criterion is a very powerful technique, and even when it is difficult to solve the gap equation in the broken phase, we can make an educated guess about the parametric dependence of the gap. This method is generally known as the Thouless criterion.

The point is that the four fermionic coupling λ_k is running with scale k in the RG language; λ_k is the coupling after modes over $k \sim \Lambda$ are integrated out. The bare coupling in the Lagrangian density takes the ultraviolet value, λ_Λ at the scale Λ , and λ_k should receive loop corrections sketched in Fig. 2 as k goes smaller.

From a one-loop diagram we can find the β function for λ_k as

$$k\partial_k \lambda_k = -\frac{\lambda_k^2 k^2}{3\pi^2}. \quad (27)$$

We can directly solve this differential equation with the initial condition of λ_Λ at $k = \Lambda$, leading to

$$\lambda_k = \frac{\lambda_\Lambda}{1 + \frac{\lambda_\Lambda}{6\pi^2}(k^2 - \Lambda^2)}, \quad (28)$$

which increases as k goes smaller. If the above is expanded in terms of λ_Λ , the geometric series indeed correspond to loop corrections in Fig. 2. In the infrared limit, $k = 0$, the denominator is $1 - \lambda_\Lambda \Lambda^2 / (6\pi^2)$. Hence, λ_k diverges at some point of k before reaching $k = 0$ if

$$\lambda_\Lambda \Lambda^2 > 6\pi^2. \quad (29)$$

The divergent coupling implies that the scattering amplitude of a particle and an anti-particle has a singularity which signifies a formation of the bound state, like a formation of the Cooper pair in

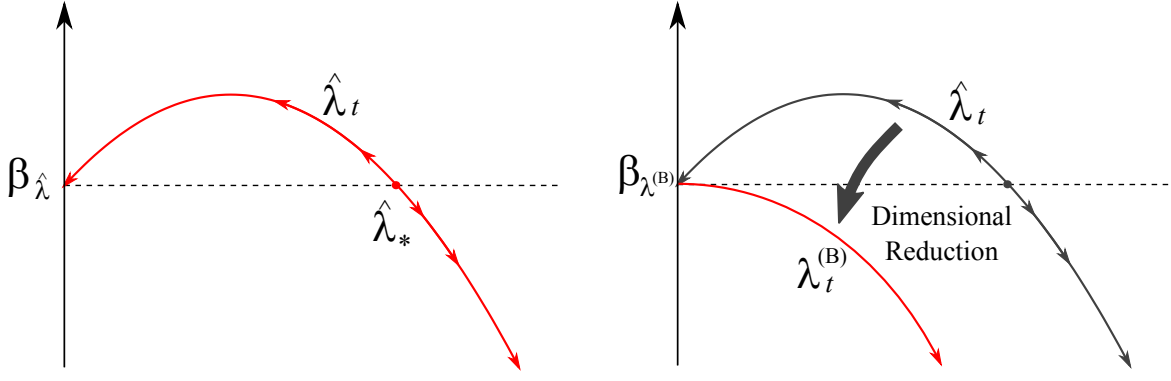


Figure 3: RG running of the coupling constant without magnetic field (left panel) and under strong magnetic field (right panel). Figures taken from Ref. [25].

superconductivity. This result is thus interpreted as the condition (23) for the scalar condensate obtained in the mean-field approximation. The discrepancy by a factor 3 supposedly comes from different cutoff schemes.

There is a more appealing way to understand the critical value of the coupling strength using the dimensionless coupling, $\hat{\lambda}_k \equiv \lambda_k k^2$. This rescaling to make λ_k dimensionless corresponds to the rescaling procedure in the conventional RG transformation. Then, the β function for the rescaled coupling is translated into

$$\beta_{\hat{\lambda}} = k \partial_k \hat{\lambda}_k = 2\hat{\lambda}_k - \frac{\hat{\lambda}_k^2}{3\pi^2}, \quad (30)$$

where the first term is added from the mass dimensionality of the coupling λ_k . Then, the zero of the β function is located at $\hat{\lambda}_* = 6\pi^2$. If the RG running is initiated from $\hat{\lambda}_\Lambda < \hat{\lambda}_*$, then $\beta_{\hat{\lambda}}$ is positive, and so $\hat{\lambda}_k$ becomes smaller as k gets smaller, which is schematically illustrated in the left panel of Fig. 3. On the other hand, if the running is launched from $\hat{\lambda}_\Lambda > \hat{\lambda}_*$, then $\beta_{\hat{\lambda}}$ is negative and $\hat{\lambda}_k$ keeps increasing with decreasing k and it eventually diverges as shown in the left panel of Fig. 3. In this way, from graphical analysis, we can identify the critical coupling in Eq. (29) from the zero of $\beta_{\hat{\lambda}}$ without solving the differential equation.

Now that we established our understanding without magnetic field, let us apply this argument to matter under strong magnetic field. We adopt the LLLA and replace the transverse phase space integration by the Landau degeneracy factor, which modifies Eq. (27) into

$$\partial_t \lambda_k = -\frac{eB}{2\pi^2} \lambda_k^2, \quad (31)$$

which can be directly solved as

$$\lambda_k = \frac{\lambda_\Lambda}{1 + \frac{\lambda_\Lambda eB}{2\pi^2} t}. \quad (32)$$

Here, $t \equiv \ln(k/\Lambda)$ ranges from 0 (at $k = \Lambda$) to $-\infty$ (at $k = 0$), and so the denominator can become zero for sufficiently large negative t if only $\lambda_\Lambda eB > 0$. This is precisely what is expected from the magnetic catalysis. As we did for $\hat{\lambda}_k$, we can define dimensionless coupling, $\lambda_k^{(B)} \equiv (eB/2\pi^2)\lambda_k$. In this case associated $\beta_{\lambda^{(B)}}$ is as simple as

$$\beta_{\lambda^{(B)}} = \partial_t \lambda_t^{(B)} = -(\lambda_t^{(B)})^2, \quad (33)$$

for which the zero is found only at $\lambda_\Lambda^{(B)} = 0$. This significant difference from Eq. (30) is attributed to the transverse phase space. For Eq. (30), by definition, the dimensionless coupling contains k^2 running with k , but for Eq. (33) the magnetic field is a more relevant scale. Then, k^2 running is lost due to

the dimensional reduction from (3+1) to (1+1) dimensional dynamics. We see that $\beta_{\lambda^{(B)}}$ in Eq. (33) is entirely negative, which means that $\lambda_{t \rightarrow -\infty}^{(B)}$ inevitably diverges for any initial λ_Λ . That is, the magnetic catalysis is again concluded from the dimensional reduction.

2.3 Inverse Magnetic Catalysis

The magnetic field has a general tendency to favor the scalar condensate, as we have discussed, but sometimes the resulting effect appears opposite. Such an exceptional situation, i.e., decreasing behavior of the scalar condensate for increasing magnetic field, is called the inverse magnetic catalysis, and the first example was found in a system at finite density [26]. If the density is high enough, in fact, it is always the case that the scalar condensate does not increase but decreases with increasing magnetic field [27], which is universally confirmed also in the RG analysis [25].

Nowadays, the inverse magnetic catalysis refers to a different realization, namely, a situation of finite temperature environment in quantum chromodynamics [28], which is a non-Abelian Yang-Mills theory with several flavors of fermions. This version of the inverse magnetic catalysis at finite temperature depends on microscopic dynamics of theory and there is no simple way to explain underlying mechanism. Nevertheless, since the recognition of the inverse magnetic catalysis posed lots of theoretical problems in the field of high-energy nuclear physics, we will go through to make some remarks on the finite-temperature inverse magnetic catalysis.

In short, the inverse magnetic catalysis can be defined as

Inverse Magnetic Catalysis: The scalar condensate is decreased if the external magnetic field is applied to the system and its strength is increased. This may happen due to interplay with other external parameters and/or other dynamics of the theory affected by the magnetic field.

2.3.1 Finite density

The scalar condensate is suppressed at finite density or finite chemical potential μ . We shall consider the effect of finite density using the NJL model again. At finite density the energy function, Eq. (21), is slightly modified as

$$E[M; \mu] = - \int_{p^2 \leq \Lambda^2} \frac{d^3 p}{(2\pi)^3} \left(|\sqrt{p^2 + M^2} - \mu| + |\sqrt{p^2 + M^2} + \mu| \right) + \frac{M^2}{2\lambda_\Lambda}. \quad (34)$$

One may notice that if M is larger than μ , there is no μ dependence at all, and this should be of course so. As long as μ is small not exceeding the mass threshold, no finite-density excitation is allowed, and thus no density effect should be visible. In what follows below we assume $\mu > M$, and then we can relax the modulus in the above energy expression, simplifying into

$$E[M; \mu] = -2 \int_{p^2 \leq p_F^2} \frac{d^3 p}{(2\pi)^3} (\mu - \sqrt{p^2 + M^2}) - 2 \int_{p^2 \leq \Lambda^2} \frac{d^3 p}{(2\pi)^3} \sqrt{p^2 + M^2} + \frac{M^2}{2\lambda_\Lambda}, \quad (35)$$

where $\mu = \sqrt{p_F^2 + M^2}$. We can easily make sure that the finite- μ correction by the first term produces a term, $p_F^2 M^2 / (12\pi^2)$, at the quadratic order in M , which energetically favors $M = 0$. When a magnetic field is imposed, the density of states is changed; continuous excited states become degenerated into the discrete Landau levels. Therefore, this finite- μ term is enhanced at larger magnetic field since the density of states is squeezed by the magnetic effect. In summary, in this case of finite density, the inverse magnetic catalysis occurs as a result of finite- μ effect enhanced by the magnetic field. There is no theoretical difficulty; the inverse magnetic catalysis is to be observed already in the mean-field approximation.

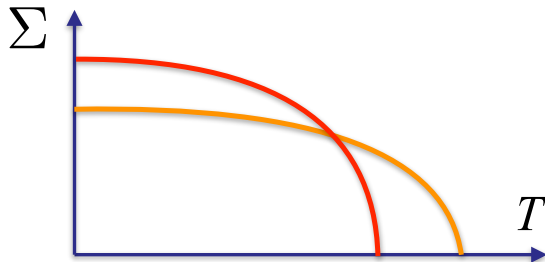


Figure 4: Schematic illustration of the change in $\Sigma(T)$ caused by the magnetic field. The orange color line is the original behavior at $B = 0$, which is pushed up to a larger value at small T . As T grows larger, however, $\Sigma(T)$ drops steeper and hits zero at smaller critical T as shown by the red color line.

2.3.2 Finite temperature

The NJL model is a relativistic cousin of the BCS theory. In this type of the theory the critical temperature, T_c , is proportional to the gap, Σ , at zero temperature, i.e., $T_c \propto \Sigma(T = 0)$, where T_c is defined by the condition, $\Sigma(T_c) = 0$. Because the magnetic catalysis with larger B pushes $\Sigma = \langle \bar{\psi}\psi \rangle$ up to a larger value, finite- T calculations using the NJL model predict that the melting temperature, T_c , where $\Sigma = 0$ is reached, monotonically increases with increasing B .

In the context of the strong interaction with quarks and gluons, such a possibility to shift T_c of the system exposed to strong B has attracted a lot of theoretical interest. Quarks and gluons interact nonperturbatively, and it is believed that the color charge is confined and the effective mass is dynamically generated in the low temperature phase. At high temperature the coupling constant runs with the energy scale and the system enters a weak-coupling regime, where both color confinement and dynamical mass generation are lost. Because these phenomena are clearly distinct, there is no necessity for two temperatures of deconfinement and melting to coincide. Numerical simulations in the first-principle theory of the strong interaction have revealed, however, that two phenomena occur almost simultaneously at one critical temperature.

This observation of the common critical temperature strongly suggests that the origins of confinement and dynamical mass generation are not distinct but should be traced back to some common microscopic mechanism in the first-principle theory. As an attempt to model a locking mechanism underlying confinement and mass generation, the NJL model has been augmented to what is called the PNJL model [29, 30] including not only Σ but also another order parameter corresponding to confinement. The PNJL model in a strong magnetic field predicted disentanglement of two phenomena; Σ is affected by the magnetic catalysis, while confinement belongs to the dynamics of gluons which are electric charge neutral, and thus the deconfinement temperature is hardly changed by the magnetic effect. If this is the case, the phase diagram of strongly interacting matter out of quarks and gluons would open a new window in which confinement is lost but fermions are still massive [31, 32].

With this background stories in mind, one may imagine how much surprised people were at numerical results from the first-principle simulation claiming that there is no disentanglement but the common phase transition temperature is lowered by a stronger magnetic field [28, 33, 34]. This means, if the order parameter Σ is plotted as a function of T for zero and nonzero magnetic field, Σ gets larger at small T , but Σ drops steeper with increasing T , as illustrated in Fig. 4.

It is nearly impossible to explain such an exotic pattern of modifications on $\Sigma(T)$ from the dynamics of mass generation alone (see Ref. [17] for a scenario closed in the chiral sector), and the coupling to confinement sector incorporated in the PNJL model is still insufficient to realize this pattern. In other words, the finite- T inverse magnetic catalysis is a serious challenge to such model studies. Clearly the PNJL model must miss something in the confinement or gluonic sector. In fact it has been known from applications to high-density matter that the gluonic potential used in the PNJL model lacks backreaction

from quark polarizations on gluon propagation (for the LLLA estimate for the polarization effect, see Ref. [35] and for the full Landau level calculation, see Refs. [36, 37]). For another nonperturbative backreaction, see Ref. [38]. These missed diagrams make the strong coupling α_s run with energy [39], as λ_k runs with k in the previous subsection. The asymptotic freedom implies that α_s is a decreasing function of B and T . Some theoretical calculations demonstrated that there may be a window of B in which T_c has a local minimum, which explains the inverse magnetic catalysis [40].

Interestingly, in the vicinity of deconfinement transition, duality between deconfined quark and confined hadronic degrees of freedom could hold. Therefore, the inverse magnetic catalysis may be approached from the hadronic side. In the hadronic phase there are many composite states of quarks which carry electric charge such as the charged pions and the proton. Such charged hadrons with nonzero spin become lighter significantly as a result of the Zeeman coupling with the magnetic field. In this way, as an extension from Ref. [41], it has been numerically confirmed that the “critical” temperature inferred from rapid changes in thermodynamic quantities is shifted down toward a smaller value for strong magnetic field [42].

2.4 Toward more realistic descriptions

We have idealized the physical setup assuming infinite volume and spatial homogeneity, but in reality, the system size, that is the size of matter distribution and/or applied magnetic field, is finite. When we discuss rotation effects later, it will be crucial to take the finite size seriously. One may think that such finite size effects are anyway small corrections, but as we will see here, qualitatively new physics arises from those analyses.

2.4.1 Solvable example of inhomogeneous magnetic field

It is generally a hard task to solve quantum field theory problems without translational invariance. Inhomogeneous electromagnetic backgrounds break translational invariance, and there is no universal algorithm to take account of such fields. Thus, if any, some theoretical exercises using analytically solvable examples would be helpful for us to sharpen our feeling about the effect of inhomogeneous fields.

One well-known solvable example is the Sauter-type potential, that is, the magnetic field is directed along the z -axis and the spatial dependence is one-dimensional along the x -axis like

$$\mathbf{B}(x) = \frac{B}{\cosh^2(kx)} \hat{\mathbf{e}}_z. \quad (36)$$

This magnetic distribution is peaked around $x \sim 0$ and the wave number k characterizes the typical scale of the spatial modulation. The Sauter-type magnetic configuration can be described by the following vector potential:

$$A^2 = \frac{B}{k} \tanh(kx), \quad (37)$$

which smoothly reduces to $A^2 = Bx$ in the limit of $k \rightarrow 0$.

The eigenvalue spectrum and the wave-functions can be found in Ref. [43] (in which the potential is called the modified Pöschl-Teller form). We will not repeat the derivation here but jump to the final results. The energy dispersion relation is, $\epsilon^2 = \lambda + p_z^2 + m^2$, where the eigenvalue λ is given, for integer $n \in [0, |\frac{1}{2} \pm \frac{eB}{k^2}| - \frac{1}{2} - \sqrt{\frac{p_y eB}{k^3}})$ (which also defines the range of p_y to keep $n > 0$) and $\tilde{n} = n + \frac{1}{2}$, to be

$$\lambda_n^\pm = p_y^2 \left[1 - \frac{(eB)^2}{(k^2 \tilde{n} - |k^2/2 \pm eB|)^2} \right] \mp eB - \left(k^2 \tilde{n}^2 - 2\tilde{n} \left| \frac{k^2}{2} \pm eB \right| + \frac{k^2}{4} \right). \quad (38)$$

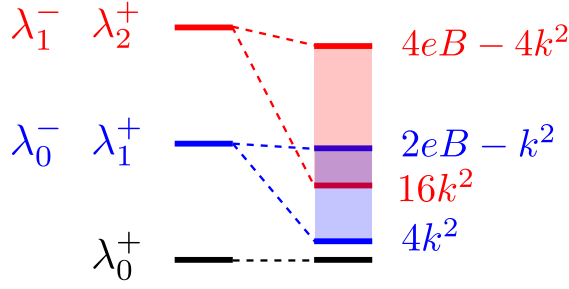


Figure 5: Schematic figure to show the eigenvalue spectra with and without spatial modulation of the magnetic field. The left is the ordinary Landau quantized spectrum. Each energy level is shifted with nonzero k . In this case the energy levels are pushed down overall.

This expression can become far simpler for small inhomogeneity if only $eB > k^2/2$ is satisfied, and then we can remove the modulus to simplify the above expression for λ_n^\pm as

$$\lambda_n^\pm = \left[1 - \frac{p_y^2 k^2}{(eB - k^2 n^\pm)^2} \right] n^\pm (2eB - k^2 n^\pm), \quad (39)$$

with $n^+ = n \in [0, \frac{eB}{k^2} - \sqrt{\frac{p_y eB}{k^3}})$ and $n^- = n + 1 \in [1, \frac{eB}{k^2} - \sqrt{\frac{p_y eB}{k^3}})$, which also constrains the possible range of p_y . We can immediately convince ourselves that the ordinary Landau quantization is recovered for $k = 0$. Then, $\lambda_n^\pm = 2eB n^\pm$ for $k = 0$ and n^\pm correspond to the spin up and down states. In particular the Landau zero mode, $n^+ = 0$, exists for one spin state only. In this case of $k = 0$ the p_y -integration yields the Landau degeneracy factor which is regularized by the system size. In other words the Landau degeneracy factor is proportional to the magnetic flux which would diverge for infinitely large systems.

The eigenvalue spectrum of Eq. (39) is very useful for us to develop our intuition about the effect of inhomogeneity. The most notable feature is that, interestingly, even though the magnetic field is inhomogeneous, the Landau zero mode, $\lambda_0^+ = 0$, exists (but the degeneracy factor could be modified). This observation could be a manifestation of the Atiyah-Singer index theorem; see Ref. [44] for more discussions. Moreover, the higher excited states are pushed down overall by inhomogeneity. Let us go a little more into concrete numbers for the low-lying states.

For homogeneous magnetic field with $k = 0$, the first Landau level is located at $\lambda_1^+ = \lambda_0^- = 2eB$ with spin degeneracy. The degeneracy with respect to p_y is lost by finite k . Here we shall assume $k^2 \ll eB$ and expand the eigen-energies in terms of k^2/eB . We then approximately obtain $4k^2 \lesssim \lambda_1^+, \lambda_0^- \lesssim 2eB - k^2$ up to the k^2 order. Therefore, the LLLA might be suspicious if k^2 is comparable to interested energy scale even though eB itself is sufficiently large, which is quite natural because the magnetic field is then damped quickly. In the same way, the second Landau level is perturbed to spread over $16k^2 \lesssim \lambda_2^+, \lambda_1^- \lesssim 4eB - 4k^2$, and so the minimal energy gap is again of order not eB but k^2 . Therefore, inhomogeneous magnetic fields soften one-particle excitation energies. If $k^2 \ll eB$, one can also perform diagrammatic perturbative expansion, as done in Ref. [45], to get some confidence about the generality of the above statement.

2.4.2 Finite size and surface effect

Instead of considering inhomogeneity in the applied magnetic field, we will turn to a different but somehow related problem in this subsection, that is, the finite size effect. We do not want to break translational invariance along the magnetic direction (i.e., the z -axis), so the simplest geometrical setup is given by the cylindrical coordinates, (r, θ, z) . Before considering the boundary effect on magnetic systems, let us first take a close look at the solutions of the free Dirac equation for $B = 0$ in the

cylindrical coordinates. For particles with positive energy, two helicity states, which can be written down explicitly as

$$u_+ = \frac{e^{-i\omega t + ip_z z}}{\sqrt{\omega + m}} \begin{pmatrix} (\omega + m)J_\ell(p_{\ell,k}r)e^{i\ell\theta} \\ 0 \\ p_z J_\ell(p_{\ell,k}r)e^{i\ell\theta} \\ ip_{\ell,k}J_{\ell+1}(p_{\ell,k}r)e^{i(\ell+1)\theta} \end{pmatrix}, \quad u_- = \frac{e^{-i\omega t + ip_z z}}{\sqrt{\omega + m}} \begin{pmatrix} 0 \\ (\omega + m)J_{\ell+1}(p_{\ell,k}r)e^{i(\ell+1)\theta} \\ -ip_{\ell,k}J_\ell(p_{\ell,k}r)e^{i\ell\theta} \\ -p_z J_{\ell+1}(p_{\ell,k}r)e^{i(\ell+1)\theta} \end{pmatrix}, \quad (40)$$

where the onshell condition is $\omega^2 = p_{\ell,k}^2 + p_z^2 + m^2$. We see that these u_\pm are simple generalization from the standard expression (6) with $\xi_\pm = (1, 0)^T, (0, 1)^T$ for u_\pm . There are, however, two major differences from Eq. (6). One is that the transverse coordinates, x, y are replaced by r, θ whose conjugate momenta are, respectively, $p_{\ell,k}, \ell$. The other is that $p_{\ell,k}$ is discretized by the system size or the cylinder radius R . That is, the discretized momentum is introduced as

$$p_{\ell,k} = \begin{cases} \xi_{\ell,k}R^{-1} & \text{for } \ell = 0, 1, \dots \\ \xi_{-\ell-1,k}R^{-1} & \text{for } \ell = -1, -2, \dots \end{cases} \quad (41)$$

where $\xi_{\ell,k}$ is the k -th zero of the Bessel function $J_\ell(x)$. We can immediately write down the anti-particle solutions using the \mathcal{C} -parity transformation, i.e., $v_\pm = i\gamma^2 u_\pm^*$ as

$$v_+ = \frac{e^{i\omega t - ip_z z}}{\sqrt{\omega + m}} \begin{pmatrix} -ip_{\ell,k}J_{\ell+1}(p_{\ell,k}r)e^{-i(\ell+1)\theta} \\ -p_z J_\ell(p_{\ell,k}r)e^{-i\ell\theta} \\ 0 \\ (\omega + m)J_\ell(p_{\ell,k}r)e^{-i\ell\theta} \end{pmatrix}, \quad v_- = \frac{e^{i\omega t - ip_z z}}{\sqrt{\omega + m}} \begin{pmatrix} -p_z J_{\ell+1}(p_{\ell,k}r)e^{-i(\ell+1)\theta} \\ -ip_{\ell,k}J_\ell(p_{\ell,k}r)e^{-i\ell\theta} \\ -(\omega + m)J_{\ell+1}(p_{\ell,k}r)e^{-i(\ell+1)\theta} \\ 0 \end{pmatrix}. \quad (42)$$

Again, it is clear that these are generalizations from Eq. (6) with appropriate choice of η_s . We also note that u_\pm have the angular momentum $j = \ell + 1/2$ and v_\pm have $-j$ along the z -axis.

Now, next, it is time to activate finite magnetic field. The positive-energy particle states with the z -component of the angular momentum, $j = \ell + 1/2$, are only slightly modified as [46]

$$u_+ = \frac{e^{-i\omega t + ip_z z}}{\sqrt{\omega + m}} \begin{pmatrix} (\omega + m)\Phi_\ell(\lambda_{\ell,k}, \frac{1}{2}eBr^2)e^{i\ell\theta} \\ 0 \\ p_z \Phi_\ell(\lambda_{\ell,k}, \frac{1}{2}eBr^2)e^{i\ell\theta} \\ ip_{\ell,k}\Phi_{\ell+1}(\lambda_{\ell,k} - 1, \frac{1}{2}eBr^2)e^{i(\ell+1)\theta} \end{pmatrix}, \quad (43)$$

$$u_- = \frac{e^{-i\omega t + ip_z z}}{\sqrt{\omega + m}} \begin{pmatrix} 0 \\ (\omega + m)\Phi_{\ell+1}(\lambda_{\ell,k} - 1, \frac{1}{2}eBr^2)e^{i(\ell+1)\theta} \\ -ip_{\ell,k}\Phi_\ell(\lambda_{\ell,k}, \frac{1}{2}eBr^2)e^{i\ell\theta} \\ -p_z \Phi_{\ell+1}(\lambda_{\ell,k} - 1, \frac{1}{2}eBr^2)e^{i(\ell+1)\theta} \end{pmatrix},$$

in which the Bessel function is upgraded to a more general special function. With the confluent hypergeometric function (Kummer's function of first kind), this upgraded functions are defined as

$$\Phi_{\ell \geq 0}(\lambda, x) = \frac{1}{\Gamma(\ell + 1)} \sqrt{\frac{\Gamma(\lambda + \ell + 1)}{\Gamma(\lambda + 1)}} x^{\ell/2} e^{-x/2} {}_1F_1(-\lambda, \ell + 1, x), \quad (44)$$

$$\Phi_{\ell < 0}(\lambda, x) = \frac{(-1)^{-\ell+1}}{\Gamma(-\ell + 1)} \sqrt{\frac{\Gamma(\lambda + 1)}{\Gamma(\lambda + \ell + 1)}} x^{-\ell/2} e^{-x/2} {}_1F_1(-\lambda - \ell, -\ell + 1, x). \quad (45)$$

The discretization condition for the transverse momenta is significantly changed as $p_{\ell,k} = \sqrt{2eB}\lambda_{\ell,k}$ and

$$\lambda_{\ell,k} = \begin{cases} \tilde{\xi}_{\ell,k} & \text{for } \ell = 0, 1, \dots \\ \tilde{\xi}_{-\ell-1,k} - \ell & \text{for } \ell = -1, -2, \dots \end{cases} \quad (46)$$

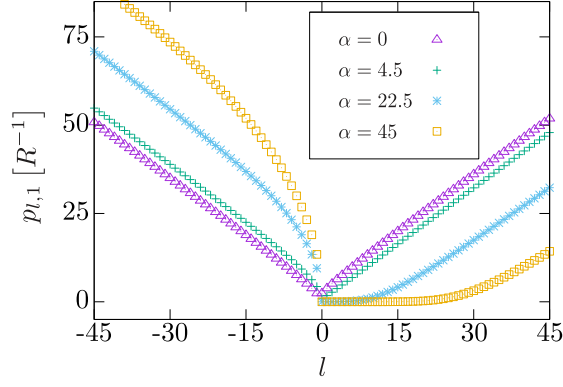


Figure 6: Lowest transverse momentum $p_{\ell,1}$ as a function of ℓ for various $\alpha = \frac{1}{2}eBR^2$. Figure taken from Ref. [46].

where $\tilde{\xi}_{\ell,k}$ is k -th zero of ${}_1F_1(-\xi, \ell + 1, \alpha)$ with $\alpha \equiv \frac{1}{2}eBR^2$. We note that α is nothing but the Landau degeneracy factor, $(eB/2\pi^2) \cdot \pi R^2$. It would be more understandable if we see Eq. (46), not as a finite- B generalization of Eq. (41), but as a finite- R generalization of the standard Landau levels. In fact, if R or α is sufficiently large, ${}_1F_1(-\xi, \ell + 1, \alpha \ll 1)$ has k -th zero at $\xi = k - 1$ for nonnegative integer ℓ .

Figure 6 shows $p_{\ell,1}$ as a function of ℓ for various α . For zero magnetic field (i.e., $\alpha = 0$), the symmetry under $\ell \leftrightarrow -\ell - 1$ is manifest. In our convention $j = \ell + \frac{1}{2}$ is the z component of the total angular momentum, and $\ell \leftrightarrow -\ell - 1$ corresponds to $j \leftrightarrow -j$. Such symmetry of sign flip of the total angular momentum is explicitly broken by the Zeeman energy from the orbital-magnetic and spin-magnetic coupling. We actually know that the Landau zero mode has only one spin state; as seen in Fig. 6, for finite α , nearly zero degenerate states of $p_{\ell,1}$ spread only in the positive- ℓ side. If B is strong enough and/or R is large enough, the boundary effects should be negligible and the Landau degeneracy of $p_{\ell,1}$ should approach α . In Fig. 6, for $\alpha = 45$ for example, the flat bottom region ends around $\ell \lesssim 30$, and so α is not yet large enough to enter the regime of the full Landau degeneracy $\sim \alpha$.

One might think that the anti-particles could be constructed by $v_{\pm} = i\gamma^2 u_{\pm}^*$ as we did previously, but this transformation does not work. In the presence of external magnetic field or vector potential in general, the \mathcal{C} -parity symmetry is explicitly broken (noting that the vector potentials are \mathcal{C} -odd), so $i\gamma^2 u_{\pm}^*$ does not satisfy the Dirac equation. The direct calculations result in

$$\begin{aligned}
 v_+ &= \frac{e^{i\omega t - ip_z z}}{\sqrt{\omega + m}} \begin{pmatrix} -ip_{-\ell-1,k} \Phi_{-\ell-1}(\lambda_{-\ell-1,k}, \frac{1}{2}eBr^2) e^{-i(\ell+1)\theta} \\ -p_z \Phi_{-\ell}(\lambda_{-\ell-1,k} - 1, \frac{1}{2}eBr^2) e^{-i\ell\theta} \\ 0 \\ (\omega + m) \Phi_{-\ell}(\lambda_{-\ell-1,k} - 1, \frac{1}{2}eBr^2) e^{-i\ell\theta} \end{pmatrix}, \\
 v_- &= \frac{e^{i\omega t - ip_z z}}{\sqrt{\omega + m}} \begin{pmatrix} -p_z \Phi_{-\ell-1}(\lambda_{-\ell-1,k}, \frac{1}{2}eBr^2) e^{-i(\ell+1)\theta} \\ -ip_{-\ell-1,k} \Phi_{-\ell}(\lambda_{-\ell-1,k} - 1, \frac{1}{2}eBr^2) e^{-i\ell\theta} \\ -(\omega + m) \Phi_{-\ell-1}(\lambda_{-\ell-1,k}, \frac{1}{2}eBr^2) e^{-i(\ell+1)\theta} \\ 0 \end{pmatrix}.
 \end{aligned} \tag{47}$$

We note that in Ref. [46] the anti-particle solutions are given with $-\ell - 1$ changed to ℓ , which means that the above states have the angular momentum $-j = -\ell - 1/2$, while such anti-particle states in Ref. [46] have $-(-\ell - 1) - 1/2 = j$. In the present choice the approximate Landau zero modes of v_{\pm} appear for negative- ℓ region since above v_{\pm} involve $p_{-\ell-1,k}$. Therefore, the angular momenta j of those nearly Landau zero modes should be positive. In this way the symmetry of particles and anti-particles is lost particularly for the Landau zero modes under strong magnetic field; the spin alignments are opposite while the total angular momenta are parallel.

Now that a complete set of wave-functions comes by, we can compute the propagator and any oper-

ator expectation values perturbatively. In fact, in Ref. [46], the scalar condensate has been calculated in the local density approximation. Then, it has been found that the magnetic catalysis is significantly strengthened near the boundary surface, $r \sim R$, due to the accumulation of large- ℓ wave-functions. Anomalous contributions near the surface may play a crucial role to fulfill global conservation of some physical charges.

3 Dynamical Problems with Electromagnetic Fields

We will explore some formalisms to cope with not only the magnetic field but also the electric field. We will start with a case with only the electric field to study the Schwinger Mechanism, and then turn on a constant magnetic field. The coexistence of the parallel electromagnetic fields would break the \mathcal{P} - and \mathcal{CP} -symmetries, and such an optical situation is a theoretically idealized setup to probe the chiral anomaly. We will introduce one idea called the chiral magnetic effect (CME) as a clear manifestation of the chiral anomaly.

3.1 Schwinger Mechanism

Quantum field theory calculus was completed in Ref. [47] and the generating functional, which is an amplitude from the past vacuum to the future vacuum, was found to acquire an imaginary part in the presence of constant electric field. The appearance of imaginary part generally signifies a kind of instability. There have been some confusions about the theoretical interpretation about the imaginary part (see Ref. [48] for judicious discussions on this issue). For some historical backgrounds together with the treatment of the Sauter-type potential, see also Ref. [5]. A comprehensive review on the Schwinger Mechanism including latest developments can be found in Ref. [6]. In this review I would not touch such a subtle argument, but I would rather prefer to formulate the same physics in terms of the particle production amplitude [49].

The particle production can occur whenever the energy-momentum conservation is satisfied and the quantum numbers are matched. In the case of the pair production, the momentum conservation can be satisfied if only the emitted particle and anti-particle are back-to-back placed. Because such particle and anti-particle carry finite energy, the external fields should inject an energy into the system. It is obviously impossible to balance the energy with homogeneous magnetic field only which gives no work on charge particles. If a pulse-like electromagnetic field externally disturbs the system, a virtual (offshell) photon from the electric field can decay into a pair of a particle and an anti-particle, and in this case, a vertex of photon, particle, and anti-particle gives a tree-level contribution to the pair production amplitude. Thus, nothing in particular is special in the pair production process.

A surprise comes from the fact that even a constant electric field can supply a finite energy, which allows for the pair production. As we will discuss later, the introduction of constant electric field assumes a time-dependent background vector potential. The time-dependence is, however, infinitesimal, and thus, the energy transfer from a perturbative process with this background field is infinitesimal. Therefore, a single scattering cannot meet the energy conservation law, but then, what about multiple scatterings? Even if the energy transfer from each scattering is infinitesimal, indeed, infinitely many scatterings eventually amount to a finite energy so that the energy conservation can be satisfied. This nonperturbative process for the pair production driven by constant electric field is called the Schwinger Mechanism, i.e.,

Schwinger Mechanism: The vacuum is unstable under constant electric field to produce pairs of a particle and an anti-particle from nonperturbative processes.

It is often said that the Schwinger Mechanism is a result of quantum tunneling. Actually, we can

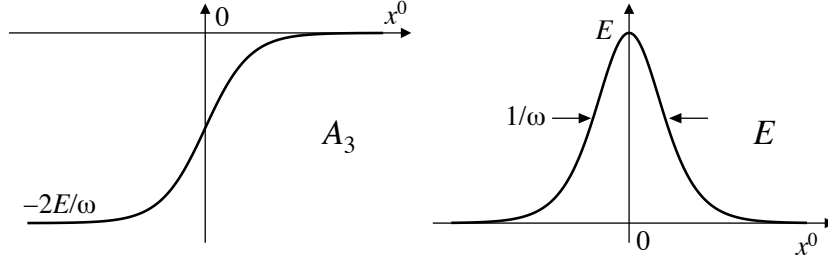


Figure 7: Profile of the vector potential and the electric field as functions of t . Figures taken from Ref. [49].

formulate a pair production as a conversion process from an anti-particle (negative-energy state) in the Dirac sea to a particle (positive-energy state). The particle and the anti-particle states are gapped by the particle mass, m , which may well be regarded as a sort of activation energy, and then the electric field is like the temperature. In this way there have been some theoretical speculations about a possible connection between the Schwinger Mechanism and thermal nature of produced particles. In fact, as we will elaborate below, the tunneling amplitude is characterized by the Bogoliubov coefficient in a way very similar to the Hawking radiation process from the blackhole (see Ref. [50] for detailed derivation of the radiated spectrum). There is a significant difference, however, in the final expressions; the rate in the Schwinger Mechanism is exponentially suppressed like $\sim \exp[-\pi m^2/(eE)]$ which is much smaller than the Boltzmann factor $\sim e^{-m/T}$ for large m .

3.1.1 Solvable example of time-dependent electric fields

Here, I would not intend to explain mathematical techniques to solve the differential equation, but using a solvable example I would present a demonstration to concretize some important concepts on the Schwinger Mechanism. The solvable example, i.e., the Sauter-type electric profile is

$$\mathbf{E}(t) = \frac{E}{\cosh^2(\omega t)} \hat{\mathbf{e}}_z, \quad (48)$$

which is realized by the following vector potential,

$$A_3(t) = \frac{E}{\omega} [\tanh(\omega t) - 1]. \quad (49)$$

It is essential to notice that A_3 in Eq. (49) takes different values in the in-state at $t \rightarrow -\infty$ and in the out-state at $t \rightarrow +\infty$, while $\mathbf{E}(t)$ in Eq. (48) goes to zero at both $t \rightarrow \pm\infty$, as displayed in Fig. 7. The background gauge potential shifts the energy dispersion relations of the in- and the out-states, respectively, as

$$E^{(\text{in})} = \sqrt{(p_3 - 2\lambda\omega)^2 + p_\perp^2 + m^2}, \quad E^{(\text{out})} = \sqrt{p_3^2 + p_\perp^2 + m^2}, \quad (50)$$

where $\lambda \equiv eE/\omega^2$ is defined.

We can quantify the particle production by computing the Bogoliubov coefficients between the in- and the out-states. For this purpose, we can solve the equation of motion from the initial condition of either a particle state or an anti-particle state, that is,

$$\psi_{\mathbf{p}}^{(1)}(t \sim -\infty) \rightarrow u(\mathbf{p}) e^{-iE^{(\text{in})}t}, \quad \psi_{\mathbf{p}}^{(2)}(t \sim -\infty) \rightarrow v(\mathbf{p}) e^{iE^{(\text{in})}t}, \quad (51)$$

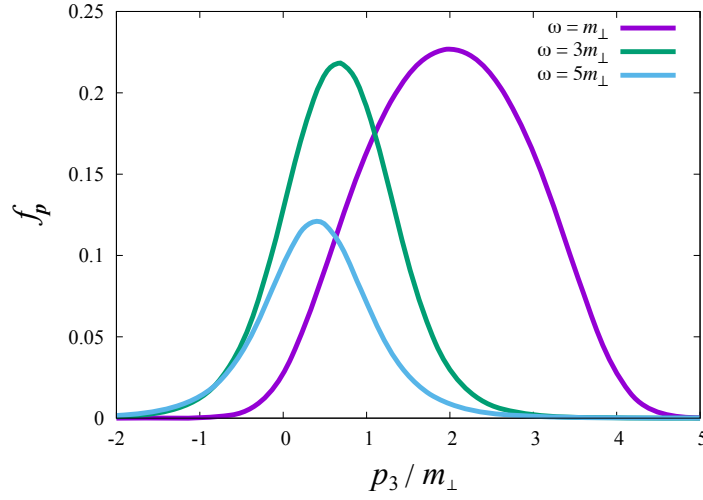


Figure 8: Produced particle distribution for $eE = 2m_\perp^2$ and various pulse parameter ω .

which evolves into

$$\begin{aligned}\psi_{\mathbf{p}}^{(1)}(t \sim +\infty) &\rightarrow A_{\mathbf{p}} u(\mathbf{p}) e^{-iE^{(\text{out})}t} - B_{-\mathbf{p}}^* v(-\mathbf{p}) e^{iE^{(\text{out})}t}, \\ \psi_{\mathbf{p}}^{(2)}(t \sim +\infty) &\rightarrow A_{\mathbf{p}}^* v(\mathbf{p}) e^{iE^{(\text{out})}t} + B_{-\mathbf{p}} u(-\mathbf{p}) e^{-iE^{(\text{out})}t}.\end{aligned}\quad (52)$$

If no electric effect is applied, there is no mixing between particles and anti-particles and thus $A_{\mathbf{p}} = 1$ and $B_{\mathbf{p}} = 0$ trivially. A nonzero $B_{\mathbf{p}}$ represents the tunneling amplitude from the anti-particle to the particle (and vice versa). With these coefficients we can identify the Bogoliubov coefficients as

$$\alpha_{\mathbf{p}} = \sqrt{\frac{E^{(\text{out})}}{E^{(\text{in})}}} A_{\mathbf{p}}, \quad \beta_{\mathbf{p}} = \sqrt{\frac{E^{(\text{out})}}{E^{(\text{in})}}} B_{\mathbf{p}}. \quad (53)$$

The produced particle distribution, $f_{\mathbf{p}}$, is given by

$$f_{\mathbf{p}} = |\beta_{\mathbf{p}}|^2. \quad (54)$$

For the Sauter-type potential the solution is known and the Bogoliubov coefficient reads [51]:

$$f_{\mathbf{p}} = \frac{\sinh[\pi(\lambda - \mu + \nu)] \sinh[\pi(\lambda + \mu - \nu)]}{\sinh(2\pi\mu) \sinh(2\pi\nu)}, \quad (55)$$

where $\mu \equiv E^{(\text{in})}/(2\omega)$ and $\nu \equiv E^{(\text{out})}/(2\omega)$. This distribution function is plotted for $eE = 2m_\perp^2$ [where $m_\perp^2 \equiv 2(p_1^2 + p_2^2 + m^2)$] as a function of p_3 in Fig. 8.

From Fig. 8 we see that the pair production rate is peaked at $p_3 = eE/\omega$ for which the above expression becomes much simpler with $E^{(\text{in})} = E^{(\text{out})}$ and thus $\mu = \nu$. At this peak position, we can take $\omega \rightarrow 0$ limit to consider constant electric field, to find that the above expression reduces to

$$f_{p_3=eE/\omega} \xrightarrow{\omega \rightarrow 0} \exp\left(-\frac{\pi m_\perp^2}{eE}\right). \quad (56)$$

This exponential factor is typical for the Schwinger Mechanism. The transverse momentum integration gives a prefactor by the phase space $\propto eE$. The remaining exponential characterizes the critical value, sometimes called the Schwinger critical electric field, whose expression is

$$(eE)_{\text{critical}} \sim \pi m^2. \quad (57)$$

I must emphasize that nothing is critical at this critical electric field. There is no phase transition nor avalanche phenomenon but the above relation is just an order estimate for the electric field necessary for a sizable amount of pair production.

3.1.2 Worldline instanton approximation

Now we would like to turn on a magnetic field on top of electric field. If these fields are constant, such a problem is solvable, though the technical details are quite complicated (see Ref. [5]). Here, we shall take a bypass, i.e., instead of getting a rigorous answer, with less efforts, it would be nice to approximate formulas correctly on the qualitative level. We further assume $\mathbf{B} \parallel \mathbf{E}$ in this section. In later discussions we will be interested in the chiral anomaly, which is optically detectable with $\mathbf{B} \cdot \mathbf{E} \neq 0$.

In this review I will entirely neglect backreaction from gauge fluctuations (see Ref. [52] for simulations with backreaction), but focus on the response of matter under fixed gauge background. Thus, it is sufficient to consider a fermionic part of the action. Because fermions enter gauge theories in a quadratic form unlike the NJL model where four fermionic interactions are assumed, we can simply identify the Dirac determinant as the full effective action, that is,

$$\Gamma[A] = -i \ln \det[\not{D} - m] = -\frac{i}{2} \ln \det \left[D^2 + m^2 + \frac{ie}{2} \sigma \cdot F \right], \quad (58)$$

where the covariant derivative is $D \equiv \partial + ieA$. From the middle to the right expression we multiplied $\gamma_5[\not{D} - m]\gamma_5 = -i\not{D} - m$ which duplicates the Dirac determinant. The last term involving the spin tensor, $\sigma^{\mu\nu} \equiv \frac{1}{2}[\gamma^\mu, \gamma^\nu]$, represents the spin-magnetic coupling.

It is straightforward to reexpress $\Gamma[A]$ in terms of the proper-time integration, as we saw in Eq. (12), using a general operator relation,

$$-\text{tr} \ln \left(\frac{\mathcal{A}}{\mathcal{B}} \right) = \int_0^\infty ds s^{-1} \text{tr} (e^{-\mathcal{A}s} - e^{-\mathcal{B}s}). \quad (59)$$

Here, \mathcal{A} is to be replaced by the Dirac operator, and $e^{-\mathcal{A}s}$ is then regarded as time evolution by a “Hamiltonian”, \mathcal{A} , with an “imaginary-time” s , which can be viewed as a quantum mechanical system evolving from x_μ at $\tau = 0$ to the same x_μ at $\tau = s$ due to the trace nature. We can adopt Feynman’s path integral representation to describe this quantum mechanical evolution for $x_\mu(\tau)$. For step-by-step transformations in detail, see Ref. [53]. After all, the derivatives or the momentum variables in the Hamiltonian are translated into $dx/d\tau$ in the Lagrangian system as

$$\Gamma[A] = \frac{1}{2} \int_0^\infty ds s^{-1} e^{-m^2 s} \oint \mathcal{D}x_\mu \exp \left\{ - \int_0^s d\tau \left[\frac{1}{4} \left(\frac{dx}{d\tau} \right)^2 + ieA \cdot \frac{dx}{d\tau} \right] \right\} \Phi[A], \quad (60)$$

where \oint represents the integration under the periodic boundary condition; $x_\mu(\tau = 0) = x_\mu(\tau = s)$. It should be mentioned that the above expression assumes the Wick rotation to Euclidean variables, (x_1, x_2, x_3, x_4) . The last part, $\Phi[A]$, corresponds to the matrix part in Eq. (58). For our special problem with $\mathbf{E} = E\hat{e}_z$ and $\mathbf{B} = B\hat{e}_z$, this last part can become factorized into the electric and the magnetic contributions as

$$\Phi[A] = \text{tr} \mathcal{P} \exp \left(\frac{ie}{2} \int_0^s d\tau \sigma \cdot F \right) = 4 \cos \left(\int_0^s d\tau eE \right) \cosh \left(\int_0^s d\tau eB \right). \quad (61)$$

Therefore, the fermionic effective action takes the following factorized form:

$$\Gamma[A] = 2 \int_0^\infty ds s^{-1} e^{-m^2 s} \mathcal{K}_E \mathcal{K}_B. \quad (62)$$

Here, introducing a dimensionless variable $u = \tau/s$, we can write down the explicit forms of the electric and the magnetic terms as

$$\mathcal{K}_E = \oint \mathcal{D}x_3 \mathcal{D}x_4 \cos \left(s \int_0^1 du eE \right) \exp \left[- \int_0^1 du \left(\frac{\dot{x}_3^2 + \dot{x}_4^2}{4s} + ieA_3 \dot{x}_3 + ieA_4 \dot{x}_4 \right) \right], \quad (63)$$

$$\mathcal{K}_B = \oint \mathcal{D}x_1 \mathcal{D}x_2 \cosh \left(s \int_0^1 du eB \right) \exp \left[- \int_0^1 du \left(\frac{\dot{x}_1^2 + \dot{x}_2^2}{4s} + ieA_1 \dot{x}_1 + ieA_2 \dot{x}_2 \right) \right], \quad (64)$$

where \dot{x}_μ represents the u -derivative of x_μ . Interestingly, for constant electromagnetic fields, these kernels can be evaluated without approximation, that is,

$$\mathcal{K}_B = \frac{eB}{4\pi} \coth(eBs), \quad \mathcal{K}_E = \frac{eE}{4\pi} \cot(eEs). \quad (65)$$

Then, the effective action can be expressed without approximation as

$$\Gamma = \frac{e^2 EB}{8\pi^2} \int_{1/\Lambda^2}^{\infty} ds s^{-1} \coth(eBs) \cot(eEs) e^{-m^2 s}. \quad (66)$$

This proper-time integration could be directly performed, which is dominated by pole contributions around $s = n\pi/(eE)$ where $\cot(eEs)$ is singular. This singularity structure implies that Γ must have a series expansion like $\sim \sum_n c_n \coth(n\pi B/E) e^{-n\pi m^2/eE}$ with some coefficients c_n of order unity.

An exact solution is of course useful, but I would rather prefer a more adaptive method applicable to a wide variety of physics problems. The worldline instanton approximation is such a flexible strategy and at the same time some interesting physical interpretation is possible. To see this, let us go back to the expression of \mathcal{K}_E in terms of x_3 and x_4 . Then, before performing the x_3 and x_4 integrations, we shall first treat the s -integration. There are two competing s dependence on the exponential; one is from the mass, $-m^2 s$, which favors smaller s , and the other is from the electric kinetic term, $-\int du (\dot{x}_3^2 + \dot{x}_4^2)/4s$, which favors larger s . One might have thought that the magnetic sector has a similar term, but we already know the answer after the integration, which behaves like $\coth(eBs) \sim 1$ for large s , and has no effect on the location of the saddle point.

We follow the physics arguments in Ref. [54]. We can find the saddle-point to approximate the s -integration at

$$s^* = \frac{1}{2m} \sqrt{\int_0^1 du (\dot{x}_3^2 + \dot{x}_4^2)}. \quad (67)$$

Then, the effective action is approximated as

$$\Gamma \approx \frac{2}{m} \oint \mathcal{D}x_3 \mathcal{D}x_4 \sqrt{\frac{\pi}{s^*}} \cos(eEs^*) e^{-S(x_3, x_4)} \mathcal{K}_B(s^*), \quad (68)$$

where we can easily get $S(x_3, x_4)$ on the exponential from this expression of s^* as

$$S(x_3, x_4) = m \sqrt{\int_0^1 du (\dot{x}_3^2 + \dot{x}_4^2)} + \int_0^1 du (ieA_3 \dot{x}_3 + ieA_4 \dot{x}_4). \quad (69)$$

We should then take care of the x_3 and x_4 integrations. If m is large, which is normally the case for the Schwinger problem, we can utilize a semi-classical approximation, i.e., the x_3 and x_4 integrations should be dominated by classical trajectories which (locally) minimize $S(x_3, x_4)$. The minimization condition is nothing but the equation of motion, and the solutions of the equation of motion are commonly referred to as “worldline instantons” for the reason explained later. It is very easy to take a variation on $S(x_3, x_4)$ to find the equation of motion as

$$\frac{m\ddot{x}_i}{\sqrt{\int du (\dot{x}_3^2 + \dot{x}_4^2)}} = ieF_{ij} \dot{x}_j \quad (70)$$

for $i, j = 3, 4$. A proper combination of these equations immediately proves $\dot{x}_3^2 + \dot{x}_4^2 = (\text{const})$, which simplifies the denominator in the left-hand side of the equation of motion. Plugging $F_{34} = iE$ (where F_{34}

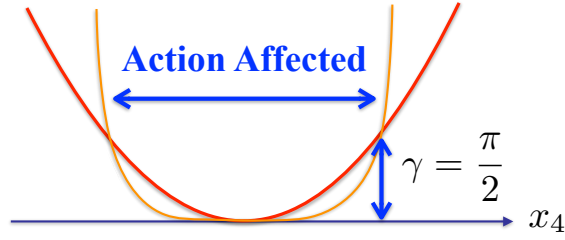


Figure 9: Schematic picture to understand the dynamically assisted Schwinger Mechanism.

is the Euclidean field strength and E is the Minkowskian physical electric field), imposing the periodic boundary condition $x_i(u=0) = x_i(u=1)$, and choosing the initial condition $x_4(u=0) = \dot{x}_3(u=0) = 0$, we can obtain the solutions of the equation of motion:

$$\bar{x}_3(u) = \frac{m}{eE} \cos(2\pi nu), \quad \bar{x}_4(u) = \frac{m}{eE} \sin(2\pi nu), \quad (71)$$

characterized by $n = 1, 2, \dots \in \mathbb{Z}^+$. These are very interesting solutions; $\bar{x}_3^2 + \bar{x}_4^2 = (m/eE)^2$ in Euclidean spacetime implies $\bar{x}_3^2 - \bar{x}_0^2 = (m/eE)^2$ in Minkowskian spacetime making hyperbolic trajectories, which are solutions under an acceleration. With these solutions, we see that the saddle point of s is located at $s_n^* = n\pi/(eE)$, which coincides with the singularities in \mathcal{K}_E . Thus, we arrive at the same conclusion of the integration dominated around $s \sim s_n^*$ though we exchanged the order of the integrations; s first and $x_{3,4}$ later or vice versa. The action with these solutions becomes:

$$\bar{S} = S[\bar{x}_3(u), \bar{x}_4(u)] = \frac{n\pi m^2}{eE}. \quad (72)$$

The prefactor in the saddle point approximation can be also calculated, and then we eventually reach the single pair production rate inferred from $w = 2\text{Im}\Gamma_M|_{n=1} = -2\text{Re}\Gamma_E|_{n=1}$. Such an expression for the particle production rate in the presence of parallel electromagnetic fields will be, in the next subsection, the key equation for our analysis on the chiral anomaly. What we learnt here is summarized as follows:

Schwinger Pair Production Rate: The rate of single pair production in the presence of parallel electric and magnetic fields is given by the formula:

$$w = \frac{e^2 EB}{4\pi^2} \coth\left(\frac{\pi B}{E}\right) \exp\left(-\frac{\pi m^2}{eE}\right). \quad (73)$$

One notable advantage in this method of the worldline instanton approximation is the generality which can be directly applied to a case with time-dependent electric perturbation. A very interesting idea has been proposed in Ref. [54]; the Sauter-type potential is infinitesimally perturbed from Eq. (48) as follows:

$$\mathbf{E}(t) = \frac{E}{\cosh^2(\Omega t)} \hat{e}_z + \frac{\varepsilon}{\cosh^2(\omega t)} \hat{e}_z, \quad (74)$$

where $\omega \gg \Omega$. The corresponding vector potential in terms of Euclidean time x_4 , up to irrelevant constants, reads:

$$A_3(x_4) = -i\frac{E}{\Omega} \tan(\Omega x_4) - i\frac{\varepsilon}{\omega} \tan(\omega x_4). \quad (75)$$

In the worldline instanton approximation, we can make use of our knowledge on classical mechanics. Even without solving the equation of motion, in classical mechanics, the energy conservation law easily derived from the equation of motion can give us an intuitive picture about the motion. In fact, the

equation of motion (70) leads to the conservation law for the sum of the kinetic and the potential energies as

$$\dot{x}_4^2 - \left(\frac{2\pi n}{eE} \right)^2 [eA_3(x_4)]^2 = (\text{const.}) \quad (76)$$

For sufficiently small Ω , the first term in $A_3(x_4)$ is well approximated by Ex_4 describing a homogeneous electric field. The second term, $(\varepsilon/\omega) \tan(\omega x_4)$ is infinitesimal for small ε except when ωx_4 approaches $\pi/2$ where $\tan(\omega x_4)$ diverges. Therefore, in this case, $[eA_3(x_4)]^2$ is an energy potential given by a superposition of a quadratic term $\propto x_4^2$ and infinite energy barriers at $\omega x_4 = \pm\pi/2$ as sketched in Fig. 9. Therefore, nothing changes from the previous case without time-dependent perturbation unless the solution of the equation of motion reaches $\omega x_4 = \pi/2$. In other words, the motion is restricted from $u = 0$ to $u^* < 1$ defined by $\omega x_4(u^*) = \pi/2$ above the threshold. The critical condition for this threshold is, $(x_4)_{\max} = (m/eE) \geq \pi/2\omega$, that is, $\gamma \equiv m\omega/(eE) \geq \pi/2$. It is extremely interesting that the action is modified even though the magnitude of the time-dependent perturbation $\propto \varepsilon$ is arbitrarily small. Actually, the exponential factor, e^{-S} appearing in the pair production formula, is suppressed above the threshold as [54]

$$S \simeq \frac{\pi m^2}{eE} \cdot \frac{2}{\pi} \left[\sin^{-1} \left(\frac{\pi}{2\gamma} \right) + \left(\frac{\pi}{2\gamma} \right) \sqrt{1 - \left(\frac{\pi}{2\gamma} \right)^2} \right] \quad \text{for } \gamma \geq \frac{\pi}{2}. \quad (77)$$

For consistency check, at the threshold $\gamma = \pi/2$, the above expression recovers the familiar Schwinger result, $S = \pi m^2/(eE)$.

3.2 Chiral Anomaly and Axial Ward Identity

In this subsection we will address an application of the Schwinger Mechanism to investigate the chiral anomaly. If the fermion mass is zero in the Dirac Lagrangian density, the axial vector current should be a conserved Nöther current on the classical level. With quantum corrections, however, the conservation law of the axial vector current is not compatible with the gauge invariance. Because the gauge symmetry must not be broken (otherwise, the renormalizability is damaged), the axial vector conservation should receive a correction which breaks down the classical level conservation law. For given gauge background the violation of the conservation law is precisely quantified in a way known as the axial Ward identity:

Axial Ward Identity: The divergence of the axial vector current j_5^μ is zero if all the fermion masses are zero on the classical level, which is modified by quantum corrections. If the theory has one Dirac fermion and Abelian gauge background fields, the violation is formulated on the level of the operator identity as

$$\partial_\mu j_5^\mu = -\frac{e^2}{16\pi^2} \epsilon^{\mu\nu\alpha\beta} F_{\mu\nu} F_{\alpha\beta} + 2m\bar{\psi}i\gamma_5\psi \quad (78)$$

In the presence of parallel \mathbf{E} and \mathbf{B} , therefore, the expectation values taken on the axial Ward identity read:

$$\partial_t \langle j_5^0 \rangle = \frac{e^2 EB}{2\pi^2} + 2m \langle \bar{\psi} i \gamma_5 \psi \rangle, \quad (79)$$

where we used $\langle j_5^i \rangle = 0$ (which can be checked by explicit calculations). This expression has an interesting interpretation. Let us assume that we can drop the last term in the chiral limit of $m \rightarrow 0$ (whose validity is far from trivial as we will argue later). Then, we can derive the above relation from a very classical consideration.

For sufficiently strong background of \mathbf{B} , the dimensional reduction occurs and the (1+1)-dimensional fermionic dispersion relations belong to the right-handed and the left-handed helicities as shown in

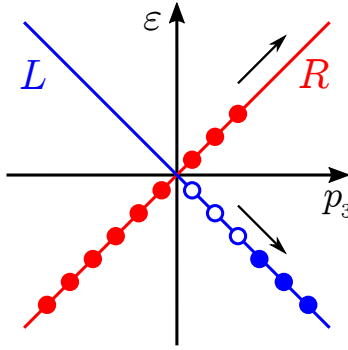


Figure 10: LLLA dispersion relations and the motion of particles/anti-particles in response to external electric field.

Fig. 10, which is essentially the same figure found in Ref. [55]. The Fermi momentum of the right-handed particles increases with E and its phase space volume gives the increasing rate of the right-handed number density, n_R , as

$$\left. \frac{\partial n_R}{\partial t} \right|_{(1+1)\text{D}} = \frac{\partial}{\partial t} \frac{eEt}{2\pi} \quad (80)$$

in reduced (1+1)-dimensional dynamics. For the left-handed particles the number density decreases, whose rate is given by the above expression with the opposite sign. The physical interpretation of Fig. 10 is transparent; under strong B together with E the pair creation produces a right-handed particle and a left-handed anti-particle, incrementing the chirality by two. Then, the total particle number is conserved, but the chirality density, $n_5 = n_R - n_L$, changes in (3+1) dimensions as

$$\frac{\partial n_5}{\partial t} = \frac{e^2 EB}{2\pi^2} \quad (81)$$

multiplied by the transverse phase space by the Landau degeneracy factor, $eB/(2\pi)$. This result perfectly agrees with Eq. (79) if n_5 is $\langle j_5^0 \rangle$.

More importantly, the above mentioned derivation of the chiral anomaly based on the pair production of a right-handed particle and a left-handed anti-particle leads to a quite suggestive relation, that is,

$$2w \simeq \partial_t \langle j_5^0 \rangle = \frac{e^2 EB}{2\pi^2} + 2m \langle \bar{\psi} i \gamma_5 \psi \rangle, \quad (82)$$

where w represents the Schwinger pair production rate (73).

3.2.1 In- and out-states

If the particle mass is zero, i.e., $m = 0$, it seems that Eq. (73) appears consistent with Eq. (73). This statement is what is frequently said in the literature, but we will see that the fact is far more complicated. To this end, we need to evaluate $\langle \bar{\psi} i \gamma_5 \psi \rangle$.

It was Schwinger [14] who first calculated $\langle \bar{\psi} i \gamma_5 \psi \rangle$ using his proper-time integration technique. In the vacuum such a pseudo-scalar condensate is vanishing, but with $\mathbf{E} \cdot \mathbf{B}$ being \mathcal{P} -odd and \mathcal{CP} -odd, a finite expectation value should be induced as $\propto \mathbf{E} \cdot \mathbf{B}$. Then, the direct calculation results in

$$\langle \bar{\psi} i \gamma_5 \psi \rangle = -\frac{e^2 EB}{4\pi^2 m} \quad (83)$$

for constant and parallel electromagnetic field without approximation. By substituting this for the axial Ward identity, we have to conclude that

$$\partial_t \langle j_5^0 \rangle = 0 \quad (84)$$

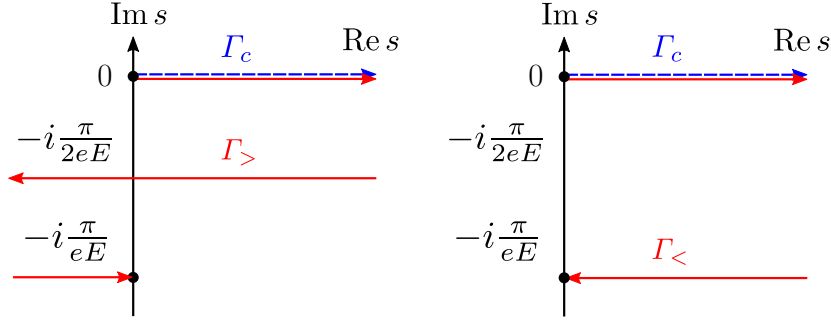


Figure 11: Contour Γ_c for $\langle \text{out} | \dots | \text{in} \rangle$ and two deformed contours, $\Gamma_>$ and $\Gamma_<$, necessary for $\langle \text{in} | \psi(x) \bar{\psi}(y) | \text{in} \rangle$. For $x_3 - y_3 > 0$ (and $x_3 - y_3 < 0$), $\Gamma_>$ (and $\Gamma_<$, respectively) is chosen. The presented paths may look different from the contours in Ref. [56] but these are equivalent. Figure taken from Ref. [57].

for any m including the $m \rightarrow 0$ limit. This result is astonishing, though this is correct! First, Eq. (84) obviously contradicts an expected relation (82). Second, the last term $\propto m$ in Eq. (78) can not always be dropped in the chiral limit of $m \rightarrow 0$. Because the condensate behaves like $\propto m^{-1}$, the m -dependence in the term $\propto m$ cancels out with the condensate and such a combination may survive. Third, the right-hand side of the axial Ward identity is zero, so that the axial vector current can be conserved. There is no way to access the chiral anomaly which existed on the operator level but disappears as an expectation value.

We can resolve this apparent puzzle once we notice that there are inequivalent ways to take the expectation values in the presence of electric field. That is, as we already learnt from Fig. 7, an electric field causes a difference between the in-state, $|\text{in}(t \rightarrow -\infty)\rangle$, and the out-state, $|\text{out}(t \rightarrow +\infty)\rangle$, which makes them distinct states. In the standard calculus of Schwinger's proper-time integration, the expectation value generally calculable in Euclidean theory corresponds to $\langle \text{out} | \dots | \text{in} \rangle$. Strictly speaking, this expectation value is not a physical observable, but an amplitude whose squared quantity is given an interpretation as a physical observable. To put it another way, $\langle \text{out} | \dots | \text{in} \rangle$ is just an expectation value in Euclidean theory which is naturally realized in the $T \rightarrow 0$ limit of finite-temperature quantum field theory. So, we may say that $\langle \text{out} | \dots | \text{in} \rangle$ is a static or spatial expectation value. We thus need to cope with $\langle \text{in} | \dots | \text{in} \rangle$ in order to access the dynamical or temporal properties of the problem.

In Ref. [57] it has been pointed out that a textbook [56] developed convenient technologies for the treatments of $\langle \text{out} | \dots | \text{in} \rangle$ and $\langle \text{in} | \dots | \text{in} \rangle$. The conventional Schwinger proper-time integration goes on Γ_c as depicted in Fig. 11, which yields $\langle \text{out} | \dots | \text{in} \rangle$. For $\langle \text{in} | \psi(x) \bar{\psi}(y) | \text{in} \rangle$ of our current interest, we should choose the deformed contours, $\Gamma_>$ for $x_3 - y_3 > 0$ and $\Gamma_<$ for $x_3 - y_3 < 0$. Therefore, the induced pseudo-scalar condensate has the following representation:

$$\lim_{y \rightarrow x} \langle \text{in} | \bar{\psi}(y) i \gamma_5 \psi(x) | \text{in} \rangle = -4i \frac{m e^2 E B}{(4\pi)^2} \int_{\Gamma_{\geq}} ds e^{-im^2 s} = -\frac{e^2 E B}{4\pi^2 m} \left[1 - e^{-\pi m^2 / (eE)} \right], \quad (85)$$

where Γ_{\geq} is either $\Gamma_>$ or $\Gamma_<$; because the integrand contains no singularity, both Γ_{\geq} give a unique answer. The above answer is consistent with the discussions also in Ref. [58] in which $\langle \text{in} | \dots | \text{in} \rangle$ quantities have been addressed for the field-theoretical computation of w , that is the left-hand side of Eq. (82) instead of the right-hand side. For the field-theoretical formulation of w , see also Ref. [49]. Now, it is clear that Eq. (82) holds with Eq. (85).

3.2.2 Optical realization of the chiral magnetic effect

We have seen that the Schwinger Mechanism describes a physical process of pair production of a right-handed particle and a left-handed anti-particle if applied B is strong enough. Apart from the backreaction, therefore, the pair production induces a chiral imbalance onto the system. It is known that such a chiral imbalance coupled with external magnetic field would be a source of exotic phenomenon in connection to the chiral anomaly.

Before the application of the Schwinger Mechanism, we shall make a flash overview of the chiral magnetic effect (CME), that is a topologically induced signature for the chiral anomaly. There are many derivations and arguments, but one of the clearest passages leading to the CME formula is the Maxwell-Chern-Simons theory (aka axion electrodynamics), that is defined by the Maxwell theory augmented with the topological θ term:

$$\mathcal{L} = -\frac{1}{4}F_{\mu\nu}F^{\mu\nu} - \frac{e^2}{16\pi^2}\theta F_{\mu\nu}\tilde{F}^{\mu\nu} + \bar{\psi}(i\not{D} - m)\psi. \quad (86)$$

The second term involving the θ angle is the Chern-Simons term, and as long as θ is constant, this θ term would not modify the equation of motion because $F_{\mu\nu}\tilde{F}^{\mu\nu}$ is a total derivative. If we assume spacetime dependent θ , however, some additional terms appear in the equation of motion and the modified Gauss and Ampère laws read [59]:

$$(\text{Gauss law}) \quad \nabla \cdot \mathbf{E} = \rho + \frac{e^2}{4\pi^2}(\nabla\theta) \cdot \mathbf{B}, \quad (87)$$

$$(\text{Ampère law}) \quad \nabla \times \mathbf{B} - \dot{\mathbf{E}} = \mathbf{j} + \frac{e^2}{4\pi^2}[\dot{\theta}\mathbf{B} - (\nabla\theta) \times \mathbf{E}]. \quad (88)$$

From this expression, we see that new terms arise in the place of \mathbf{j} which can be identified as new contributions to the current. One might think that such induced terms could be a fictitious current like Maxwell's displacement current, $\dot{\mathbf{E}}$, as questioned in Ref. [7]. To answer this question, we should consider how the charge conservation holds for a finite system; actually, charge density $\propto (\nabla\theta) \cdot \mathbf{B}$ emerges in a perfectly consistent way with the current $\propto \dot{\theta}\mathbf{B}$, which means that this new current $\propto \dot{\theta}\mathbf{B}$ is a genuine current unlike Maxwell's displacement current. Changing the notation from $\dot{\theta}$ to μ_5 , we arrive at the standard CME formula [60] (for a pretty complete list of preceding works including Vilenkin [61] and Giovannini-Shaposhnikov [62], see Ref. [4]):

Chiral Magnetic Effect: A nonzero chirality imbalance is induced by $\dot{\theta} = \mu_5$, which is coupled with external magnetic field, \mathbf{B} , leading to an electric current parallel to \mathbf{B} as

$$\mathbf{j}_{\text{CME}} = \frac{e^2}{4\pi^2}\mu_5\mathbf{B} \quad (89)$$

This is a formula for a single fermion contribution. If the theory has multiple species of fermions, the above current is multiplied by the fermionic degrees of freedom. Interestingly, the formula is insensitive to the fermion mass, and it is independent of the temperature, as should be so for the quantum anomaly.

An intuitive view point to understand the CME is picturized in Fig. 12. By definition, the right-handed particles have the spin and the momentum in parallel directions, while the left-handed particles have anti-parallel spin and momentum. The spin direction is aligned along the magnetic field as shown in Fig. 12, which simultaneously fixes the momentum direction. A nonzero μ_5 induces unbalanced chirality density, $n_5 = n_R - n_L \neq 0$, and thus, a combination of $n_5 \neq 0$ and the spin-magnetic correlation generates a net current along the magnetic direction. Such an electric current $\parallel \mathbf{B}$ is inherently anomalous that does not exist in classical electrodynamics in which the magnetic field does not transfer any work on

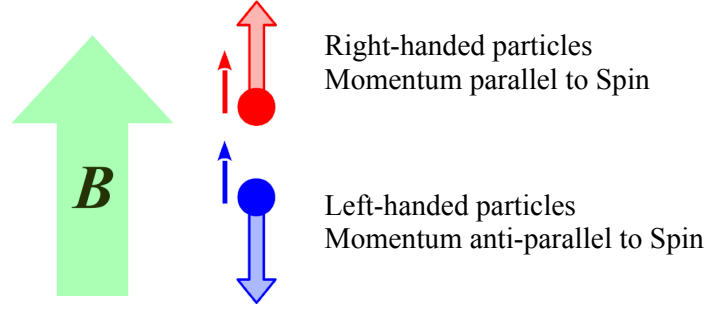


Figure 12: A classical picture for the CME under a strong magnetic field. The spin is aligned to the magnetic direction, which uniquely fixes the direction of the momentum depending on whether particles are right-handed or left-handed. Then, if there is an excess of either right-handed or left-handed particles, a net electric current flows along the applied magnetic field.

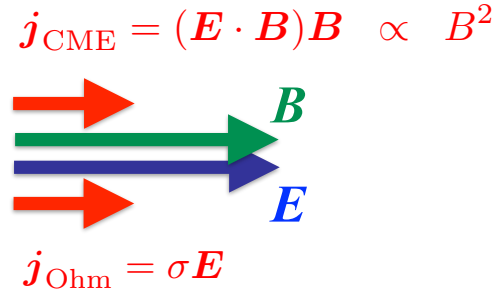
charged particles. The energy is supplied by μ_5 or in other words the driving force is provided by time-dependent θ .

Regarding the physical interpretation of the formula, there have been controversies. Some came from the derivation presented in Ref. [60]; the thermodynamic potential $\Omega[\mathbf{A}]$ was calculated on background vector potential \mathbf{A} , magnetic field \mathbf{B} , and chiral chemical potential μ_5 , and the current was estimated from $\mathbf{j} \propto \delta\Omega/\delta\mathbf{A}$. Nothing is wrong about this procedure, but strangely, this derivation implies the existence of the permanent current even in equilibrium! A state with current should be, even if it is time independent, a steady state out of equilibrium. In short, in equilibrium, the CME current must be prohibited by definition of equilibrium. Here, one must not be confused with the argument in Ref. [63], though the claim itself sounds similar. The important message from Ref. [63] is that the CME current does not exist in solid state systems where there is no Dirac sea (from which the anomaly arises) and also the surface term cancels out with periodic boundary condition (see also Ref. [64] for related discussions). In this sense, the statement of Ref. [63] is the same claim but made under tighter constraints, not applied to continuous quantum field theory. What I am emphasizing here is that even in continuous quantum field theory the CME current cannot be permitted in equilibrium.

A sort of consensus has been built in the community, that is, a nonzero μ_5 is the trick to emulate a steady state using an equilibrium language. More concretely, μ_5 should be zero in true equilibrium situation, and the introduction of nonzero μ_5 forces the system to be out of equilibrium. Such an interpretation physically makes sense, but as long as μ_5 is introduced by hand, there is no way to turn off effects to mimic off-equilibrium. One way to cure this situation is to take account of the relaxation process of μ_5 decaying toward zero as the time goes.

Another (and more well-founded) theoretical approach would be to abandon using μ_5 . The role played by μ_5 is to inject an energy imbalance between the right-handed particle sector and the left-handed particle sector. We have already argued that the Schwinger Mechanism under strong magnetic field leads to exactly such chirality imbalance. Hence, we can just impose an external \mathbf{E} so that $\mathbf{E} \cdot \mathbf{B} \neq 0$ can replace μ_5 . This idea was first proposed in Ref. [65] and analytical formulas based on the identification of Eq. (82) have been derived for a geometry of \mathbf{E} and \mathbf{B} making an angle less than $\pi/2$ (i.e., \mathbf{B} has both components $\parallel \mathbf{E}$ and $\perp \mathbf{E}$). We have already seen that, surprisingly, the Euclidean expectation values make the right-hand side of the axial Ward identity vanishing, which also means that the CME current is vanishing then. Now, we understand that this must be so; the CME current should be indeed vanishing for static systems described in Euclidean formulation, as was clarified in Ref. [57].

Later on, the simple idea of Ref. [65] was further simplified in Ref. [66]; no angle between \mathbf{E} and \mathbf{B} is necessary, but only the parallel $\mathbf{E} \parallel \mathbf{B}$ is sufficient to probe the CME current as sketched in

$$j_{\text{CME}} = (\mathbf{E} \cdot \mathbf{B})\mathbf{B} \propto B^2$$


$$j_{\text{Ohm}} = \sigma \mathbf{E}$$

Figure 13: Simplest setup to observe the CME current in terms of the negative magnetoresistance.

Fig. 13. The idea is the following. The simplest optical setup is just to impose an external magnetic field only on chiral material along which a finite voltage is applied so that an electric current flows. Then, the electric field should be present there according to Ohm's law, i.e., $\mathbf{j}_{\text{Ohm}} = \sigma \mathbf{E}$ where σ denotes the Ohmic electric conductivity. Because of the electromagnetic background, a finite chirality is pumped up as $n_5 \propto \mathbf{E} \cdot \mathbf{B}$ as deduced from Eq. (73), which means that $\mu_5 \propto \mathbf{E} \cdot \mathbf{B}$ is anticipated. Then, the CME formula with $\mu_5 \propto \mathbf{E} \cdot \mathbf{B}$ implies the CME current, $\mathbf{j}_{\text{CME}} \propto (\mathbf{E} \cdot \mathbf{B})\mathbf{B} \propto B^2$. From this relation we can deduce that the electric conductivity σ_{CME} associated with the CME current has peculiar magnetic dependence $\propto B^2$. The experimentally observed current should be a superposition of $\mathbf{j}_{\text{Ohm}} + \mathbf{j}_{\text{CME}} = (\sigma + \sigma_{\text{CME}})\mathbf{E}$, where σ is assumed to have only minor dependence on \mathbf{B} . Therefore, if an anomalous component of the electric conductivity increasing with B^2 or equivalently the electric resistivity decreasing with B^{-2} is confirmed, it would be a clear experimental signature for σ_{CME} and thus the chiral anomaly. Such a behavior of the resistivity suppressed as B^{-2} is especially referred to as the “negative magnetoresistance” in the literature. Finally, let us make a remark on the asymptotic B dependence in the strong- B limit. In the above discussion a relaxation process of the produced chirality is implicitly assumed; otherwise, the chirality diverges over a long time. Actually in Ref. [66] the relaxation time approximation is adopted in the framework of the chiral kinetic theory, and also in Ref. [67] that is the very first report of the experimental observation of the negative magnetoresistance, a relaxation time is introduced in a Drude-type picture. Then, such quadratic dependence of the conductivity or resistivity is predicted if the relaxation time is B independent. In reality, however, the relaxation time or the microscopic scattering process is significantly affected by B -dependent phase space volume. A complete field-theoretical computation of the electric conductivity including higher Landau levels have revealed that the physical asymptotic dependence on B is not quadratic but linear [68].

4 Phenomena induced by Rotation

In many physics problems the angular momentum causes a phenomenological consequence analogous to the magnetic effect. In fact rotating chiral matter would exhibit a current which looks similar to the CME current. This effect to generate rotation induced axial current is called the chiral vortical effect (CVE). Because the axial current operator is nothing but the spin operator in the relativistic language, the CVE could be regarded as a transport process from the mechanical rotation into the spin or the magnetization, which may well be a relativistic extension of the Barnett effect. Then, it would be a natural question to think of another relativistic extension, namely, the Einstein–de-Haas effect. These are new subjects and so we will only briefly look over speculative ideas.

Furthermore, recently, there are many interesting works to discuss the ground state properties affected by rotation effects, see Ref. [69] for a phase diagram, Ref. [70] for the scalar condensate, Ref. [71] for the pion condensation, etc. These are all exciting developments, but in this review, we will stay with simpler physics problems only.

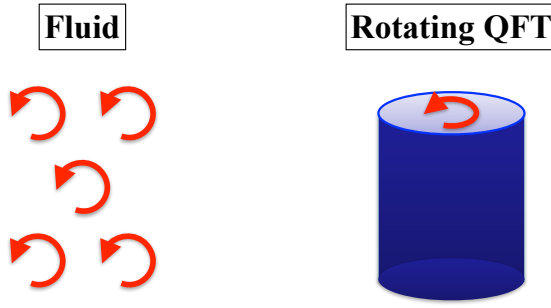


Figure 14: Two treatments of rotational effects; (left) local vorticity vector characterizes the distribution of $\nabla \times \mathbf{u}$ where \mathbf{u} is a fluid velocity vector and (right) rigidly rotating object treated in a rotating frame gives global rotation but needs boundary not to break causality.

4.1 Rotating Chiral Fermions

Rotation effect has been well understood in some fields of physics such as nuclear physics in which all deformed nuclei must rotate to restore broken symmetry in a finite system. Such a quantum system in a rotating frame can be described by the cranking Hamiltonian, that is, the Hamiltonian shifted by a cranking term, $\mathbf{j} \cdot \boldsymbol{\omega}$, where $\boldsymbol{\omega}$ is the angular velocity vector and j is the total angular momentum. Such an energy shift can be identified as an effective chemical potential. In this sense, a finite rotation has dual aspects as a magnetic counterpart and a finite-density counterpart. In particular the analogy between rotation and finite density has been pursued in Ref. [72] in which the rotation-induced inverse magnetic catalysis has been found. From this analogy the phase diagram as a function of the temperature vs. the rotation angular velocity can be considered, and similarity to the conventional phase diagram as a function of the temperature vs. the chemical potential has been verified in Ref. [69].

To incorporate rotational effect, two technically distinct treatments are commonly adopted; one method is a description with local vorticity vector of a fluid, and the other is with global rotation via coordinate transformation to a rotating frame, as schematically drawn in Fig. 14. Each has an advantage and a disadvantage. Because the vorticity is a local quantity, the former method has no necessity to be put in a finite sized system. Without the boundary, however, there is no simple way to take account of the orbital angular momentum (see Refs. [73] for examples of theoretical attempts for spinning hydrodynamics). The latter is in this sense more convenient in order to consider the orbital angular momentum of a finite system. Unlike the former fluid description, however, the center of rotation and the boundary at the surface make physical quantities inhomogeneous depending on the radial distance.

Here, I would stress that two treatments should be equivalent if the same physical system is considered. It is well known that, for example, a rotating superfluid forms a lattice of vortices which carry a quantized angular momentum, and as the rotating velocity of the superfluid increases, the number of vortices gets larger, and eventually approaches the rigid rotor limit. In this way, a uniform distribution of vorticity vector should amount to the global rotation.

4.1.1 Field-theoretical treatments

I prefer the treatment using quantum field theory in a rotating frame, which enables us to perform rather brute-force calculations. The derivation of the rotation induced current is quite suggestive, having similarity to the Casimir effect to some extent, which is worth discussing.

The starting point of field-theoretical computation is the Dirac equation in a rotating frame. For free Dirac fermion the Lagrangian density reads:

$$[i\gamma^\mu(\partial_\mu + \Gamma_\mu) - m]\psi = 0, \quad (90)$$

where $\Gamma_\mu = -\frac{i}{4}\omega_{\mu ij}\sigma^{ij}$ with $\sigma^{ij} = \frac{i}{2}[\gamma^i, \gamma^j]$. The spin connection is $\omega_{\mu ij} = g_{\alpha\beta}e_i^\alpha(\partial_\mu e_j^\beta + \Gamma_{\mu\nu}^\beta e_j^\nu)$ given in terms of the metric and the Vierbine. In a frame rotating along the z -axis, the metric involves the angular velocity ω as

$$g_{\mu\nu} = \begin{pmatrix} 1 - (x^2 + y^2)\omega^2 & y\omega & -x\omega & 0 \\ y\omega & -1 & 0 & 0 \\ -x\omega & 0 & -1 & 0 \\ 0 & 0 & 0 & -1 \end{pmatrix}. \quad (91)$$

The corresponding Vierbine is not uniquely fixed but can be chosen as

$$e_0^t = e_1^x = e_2^y = e_3^z = 1, \quad e_0^x = y\omega, \quad e_0^y = -x\omega. \quad (92)$$

With this choice we can explicitly write down the free Dirac equation in the following way:

$$\left\{ i\gamma^0 \left[\partial_t + \omega \left(-x\partial_y + y\partial_x - \frac{i}{2}\sigma^{12} \right) \right] - i\gamma^1\partial_x - i\gamma^2\partial_y - i\gamma^3\partial_z - m \right\} \psi = 0. \quad (93)$$

Interestingly, though the metric contains ω^2 term, the Vierbine is linear and this above equation is also linear in terms of ω . The physical interpretation of terms coupled with ω is evident. As explained above, the cranking term shifts the Hamiltonian or the energy by $\mathbf{j} \cdot \boldsymbol{\omega}$, and the quantity with parentheses is nothing but the total angular momentum. This energy shift is essential to understand various physics phenomena, like a critical velocity for the superfluid vortex.

4.1.2 Chiral vortical effect

It was Vilenkin who found that the expectation value of the axial vector current is something finite proportional to ω [74], which was reconfirmed by more field-theoretical frameworks later [75, 76]. The statement itself is quite nontrivial, and moreover, the derivation is extremely interesting. Before looking at the derivation, let us see the final expression:

Chiral Vortical Effect: Axial vector current is induced by a combination of rotation with the angular velocity ω and chiral matter characterized by fermionic thermal distribution function $f_F(\varepsilon_p)$. For the distribution functions with chemical potentials $\mu_{R/L}$ for the right-handed and the left-handed fermions, the CVE formula reads:

$$\mathbf{j}_{R/L} = \mp \boldsymbol{\omega} \int \frac{d^3p}{(2\pi)^3} f'_F(\varepsilon_p; \mu_{R/L}), \quad (94)$$

where $f'_F(\varepsilon_p)$ represents the derivative of $f_F(\varepsilon)$ with respect to ε_p .

The structure of the formula may look similar to the CME current; the CVE current is proportional to $\boldsymbol{\omega}$ and the CME current to \mathbf{B} , which are both not explainable in classical physics. However, there is an essential difference. The CME appears from the vacuum fluctuation and there is no contribution from the finite- T part, but the CVE originates from the matter part only. The above formula is further simplified for $m = 0$ as

$$\mathbf{j}_{R/L} = \pm \left(\frac{T^2}{12} + \frac{\mu_{R/L}^2}{4\pi^2} \right) \boldsymbol{\omega} \quad (95)$$

which is perhaps the most well recognized expression in the literature.

Now we shall take a closer look at the derivation. As seen from the Dirac equation (93), the rotation effect lies in an energy shift by $\mathbf{j} \cdot \boldsymbol{\omega}$, and so the propagator S in a rotating frame is obtained from S_0 in the inertial frame with the shift operator as

$$S(\mathbf{x}, \mathbf{x}', p_0) = e^{\boldsymbol{\omega} \cdot \mathbf{j} \frac{\partial}{\partial p_0}} S_0(\mathbf{x}, \mathbf{x}', p_0), \quad (96)$$

where $\mathbf{j} = \mathbf{L} + \frac{1}{2}\mathbf{\Sigma}$ with the spin vector defined as $\Sigma^i \equiv \frac{1}{2}\epsilon^{ijk}\sigma^{jk}$. It should be noted that the above propagator is Fourier transformed only for the temporal component, for \mathbf{L} is \mathbf{x} dependent. We are now estimating the axial vector expectation value, $\text{itr}[\gamma^\mu\gamma_5 S(x, x)]$, which involves γ_5 . This trace is vanishing unless three γ matrices come along from S . The free propagator, S_0 , is proportional to one γ matrix, and two more are necessary from the shift operator, $e^{\omega \cdot \mathbf{j} \frac{\partial}{\partial p_0}}$. For small ω we can expand the shift operator in terms of ω and then the first remaining term is thus the spin part with $\mathbf{\Sigma}$ which contains two γ matrices. Therefore, the expectation value of the axial vector current reads:

$$j_5^\mu = -\text{itr}[\gamma^\mu\gamma_5 S(x, x)] = -i\omega \text{tr}\left[\gamma^\mu\gamma_5 \frac{1}{2}\Sigma \frac{\partial}{\partial p_0} S_0(\mathbf{p}, p_0)\right] + O(\omega^2). \quad (97)$$

Here, the first tr is taken in configuration space and the second in momentum space. Using the trace property, $\text{tr}[\gamma_5\gamma^\mu\gamma^\nu\gamma^\rho\gamma^\sigma] = 4i\epsilon^{\mu\nu\rho\sigma}$, and introducing the angular velocity tensor, $\omega^{ij} = \frac{1}{2}\epsilon^{ijk}\omega_k$ (in fact, the angular velocity is originally a two-rank tensor like the angular momentum), we can simplify the above expression as

$$j_5^\mu = -i\epsilon^{\mu\alpha\beta\nu}\omega_{\alpha\beta} \int^T \frac{d^4p}{(2\pi)^4} \frac{\partial}{\partial p_4} \frac{p_\nu}{p^2 + m^2}. \quad (98)$$

Here, a finite- T field theory is assumed, and p_0 is Wick rotated to the Matsubara frequency, $p_4 = 2\pi nT$. This expression is quite remarkable. If p_4 were a continuous variable (at $T = 0$) and if there were no surface contribution (at $\mu = 0$), the integral is trivially zero. In other words, the term $\propto \mu^2$ in Eq. (95) emerges from the edges of the momentum integration, which is a common typical feature of quantum anomaly. The term $\propto T^2$, in contrast, seems to have a rather different origin; this is nonzero because of a finite discrepancy between a continuous integral and a discrete sum, which is more reminiscent of the Casimir energy!

As a matter of fact, it is still under theoretical disputes whether the T^2 -term in the CVE formula is related to quantum anomaly or not. From the group theoretical structure, in Ref. [77], a connection to the mixed gravitational chiral anomaly was conjectured, which was followed by holographic studies [78, 79, 80]. However, the coefficient of the T^2 -term is not anomaly protected, while the μ^2 -term is not renormalized by the interaction [81]. Besides, it has been clarified that the CVE coefficient is fixed by the mixed global anomaly, not the perturbative anomaly [82], but this itself is not so surprising because the T^2 -term is a pure finite- T effect which is in any case traced back to the compactification. For discussions from the point of view of hydrodynamics, see Refs. [83, 84]. A more hint for a possible relation to the gravitational anomaly may well be available from the calculation including spatial curvature as well as rotation. It is a straightforward generalization to include the effect of curved space into the above calculation, which after some algebra leads to [85]

$$\mathbf{j}_{R/L} = \pm \left(\frac{T^2}{12} - \frac{m^2}{8\pi^2} - \frac{R}{96\pi^2} \right) \boldsymbol{\omega}, \quad (99)$$

apart from the chemical potential terms, together with a mass correction up to m^2 order. The last term is purely geometrical and its coefficient not surprisingly coincides with that of the Chern-Simons current associated with the gravitational anomaly. The second term is a mass correction from the distribution function in Eq. (94). Suggestively, this m^2 -term from the CVE formula is perfectly consistent with what is expected from the chiral gap effect, that is, a mass shift by the curvature as $m^2 \rightarrow m^2 + R/12$ as found in Ref. [86]. In this way, through the m^2 -term, we could observe at least an indirect relationship between the T^2 -term in the CVE current and the gravitational anomaly.

4.2 Floquet Theory

The CVE is as interesting as the CME, but controlling physical rotation in laboratory would require a delicate design for experimental machineries. Here, we will see that, not the CVE itself, but some quite

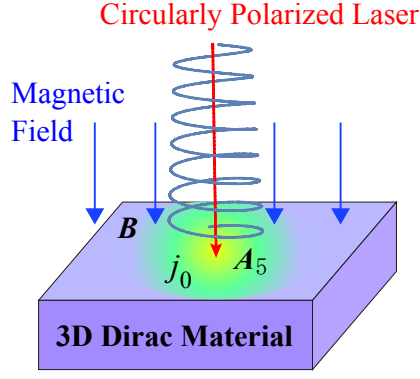


Figure 15: Chiral pumping effect: chiral matter exposed to circularly polarized transverse electric field together with longitudinal magnetic field.

similar phenomena would be accessible by means of circularly polarized electromagnetic fields. In fact, such an optical setup has been intensely investigated in quantum optics and laser physics (and also in the quantum field theory context too, see Ref. [87] for a recent work), and it has been known that the Floquet theory is a powerful tool (for a pedagogical review on the Floquet theory, see Ref. [9]).

The Floquet theory is a temporal version of the Bloch theorem, that is:

Floquet Theory: Quantum states for a time periodic Hamiltonian with a periodicity T , satisfying $H(t + T) = H(t)$, are described by wave-functions in a form of

$$\psi_n(t) = u_n(t) e^{-i\varepsilon_n t}, \quad (100)$$

with periodic Floquet modes, $u_n(t + T) = u_n(t)$.

For the time-periodic system the one-cycle time evolution defines an effective Hamiltonian, called the Floquet Hamiltonian, given by

$$e^{-iT H_{\text{eff}}} = \mathcal{T} \exp \left[-i \int_0^T dt H(t) \right]. \quad (101)$$

With this effective Hamiltonian the dynamical problem is reduced to a static one. The idea of the Floquet engineering is to design H_{eff} that has desired properties on a finite time scale. For example spacetime dependent θ as in Eq. (86) could be engineered, which would open an opportunity to study induced terms in Eqs. (87) and (88) experimentally.

4.2.1 Rotating frame and Magnus expansion

Here is one example of the Floquet engineering to induce z dependent θ , which is equivalent to an axial vector potential $\mathbf{A}_5 = \beta \hat{\mathbf{e}}_z$. In electromagnetism, of course, there is no such axial vector potential, and we will see a theoretical benefit from the Floquet theory with this demonstration presented in this subsection.

Let us consider a circularly polarized electric field with the following vector potential:

$$A_x = \frac{E}{\omega} \cos(\omega t), \quad A_y = \frac{E}{\omega} \sin(\omega t). \quad (102)$$

The corresponding Hamiltonian is periodically time-dependent, i.e.,

$$H = \gamma^0 \boldsymbol{\gamma} \cdot \mathbf{p} + \gamma^0 m - e \gamma^0 \boldsymbol{\gamma} \cdot \mathbf{A} = \underbrace{\gamma^0 \boldsymbol{\gamma} \cdot \mathbf{p} + \gamma^0 m}_{H_0} - \underbrace{\frac{eE}{\omega} \gamma^0 \gamma^- e^{i\omega t}}_{H_-} - \underbrace{\frac{eE}{\omega} \gamma^0 \gamma^+ e^{-i\omega t}}_{H_+} \quad (103)$$

with $\gamma^\pm \equiv \frac{1}{2}(\gamma^1 \pm i\gamma^2)$. In the above the whole Hamiltonian is split into a static part, H_0 , and the positive- and negative-frequency parts, H_\pm . The Floquet effective Hamiltonian can be systematically obtained by the ω^{-1} expansion if ω is large enough (only for which the Floquet theory physically makes sense; otherwise, the temperature diverges without prethermalization [88]). Then, there is a formula known as the Magnus expansion [89], from which we can read the first expanded term up to $O(\omega^{-1})$ using the above notation, H_0 and H_\pm , as

$$H_{\text{eff}} \simeq H_0 + \frac{1}{\omega}[H_-, H_+] = \gamma^0 \boldsymbol{\gamma} \cdot \mathbf{p} + \gamma^0 m - \beta \gamma^0 \gamma^z \gamma_5 \quad (104)$$

with $\beta \equiv (eE)^2/\omega^3$. Now we understand that we can regard this last term as an induced axial vector potential, $\mathbf{A}_5 = \beta \hat{\mathbf{e}}_z$.

Because $2\mathbf{A}_5$ is transformed into $\nabla\theta$, the modified Gauss law (87) indicates that a finite charge density is pumped up (i.e., chiral pumping effect) as

$$\rho_{\text{induced}} = \frac{e}{2\pi^2} \beta B, \quad (105)$$

coupled with a magnetic field, $\mathbf{B} = B\hat{\mathbf{e}}_z$, which can be derived also from direct calculations [90].

The effect of circularly polarized electric field mimics rotational effect, which can be better understood in the following manner. Instead of a combination of circularly polarized electric field and static magnetic field, let us consider just a rotating magnetic field which produces periodically driven potential. We can eliminate time dependence by the coordinate transformation:

$$x \rightarrow (\cos \omega t)x - (\sin \omega t)y, \quad y \rightarrow (\cos \omega t)y + (\sin \omega t)x. \quad (106)$$

Then, the Floquet transformation of the basis,

$$\psi \rightarrow \exp(\gamma^1 \gamma^2 \omega t/2) \psi, \quad (107)$$

with the replacement of $\gamma^i \rightarrow \gamma^\mu$ with the Vierbine reduces the problem into a static one characterized by the transformed Lagrangian density:

$$\mathcal{L} = \bar{\psi} \left[i\gamma^0 \partial_t + i\gamma^1 \partial_x + i\gamma^2 (\partial_y - ieBx) + i\gamma^3 \partial_z + \frac{\omega}{2} \gamma^3 \gamma_5 \right] \psi. \quad (108)$$

Now, we see that a rotating magnetic field is transformed into a static one, as expected from the frame change, and the effect is not only that but also the transformation gives rise to a new term, which can be identified with the axial vector potential corresponding to $\beta = \omega/2$, leading to [91]

$$\rho_{\text{induced}} = \frac{eB\omega}{4\pi^2}. \quad (109)$$

In this case the above result assumes no approximation, which makes a sharp contrast to the previous calculation based on the Magnus expansion. This exactness of resulting ρ_{induced} is explained by the anomaly nature [92].

4.2.2 Interpretation as an artificial electric field

The Floquet theory has an interesting interpretation in physics, as argued in a review [93], which has much to do with the main subject of this article. We will briefly look over the basic idea of what is called Sambe space [94].

The periodic Hamiltonian has a Fourier expanded form,

$$H(t) = H(t+T) = \sum_{n=-\infty}^{\infty} H_n e^{-in\omega t} \quad (110)$$

with $\omega = 2\pi/T$. The Floquet state having a quasi-energy, ε_α , can be also Fourier expanded as

$$u_\alpha(t) = \sum_{n=-\infty}^{\infty} u_{\alpha n} e^{-in\omega t}. \quad (111)$$

Then, the eigenvalue equation to determine the quasi-eigenenergy and the Floquet basis states reads:

$$\sum_m (H_{n-m} - n\omega\delta_{mn}) u_{\alpha m} = \varepsilon_\alpha u_{\alpha n}. \quad (112)$$

In Floquet picture this eigenvalue equation is given an interesting interpretation. The matrix representation of the quasi-energy operator in the left-hand side has diagonal components, H_0 , $H_0 \pm \omega$, $H_0 \pm 2\omega, \dots$, and these states are communicated by off-diagonal interactions, $H_{\pm 1}$, $H_{\pm 2}, \dots$. Then, along the Floquet direction labeled by m , the diagonal Hamiltonian has an energy slope by $m\omega$. If we regard this Floquet direction as an extra spatial axis, we can identify the energy shift, $m\omega$, as a coordinate dependent static potential. Therefore, the slope of the energy shift is nothing but a static electric field $\propto \omega$ (one more mass dimension should be compensated by “lattice spacing” which is arbitrary in the present description). This picture of fictitious electric field is useful, for example, to think of topological aspects in Floquet systems.

It would be an fascinating possibility to realize effects equivalent to $\mathbf{E} \cdot \mathbf{B} \neq 0$ in (3+1) dimensions without using \mathbf{E} but with just time periodic perturbations onto a system in (2+1) dimensions. Such a connection between the Floquet system and the finite- \mathbf{E} system should deserve more investigations from both theoretical and experimental sides.

4.3 Relativistic Gyromagnetic Effects

The CVE is an axial vector current induced by rotation, as we have already seen, and the axial vector is translated to a spin expectation value in the non-relativistic limit. Actually, in non-relativistic theories, it is a well established notion that a finite orbital angular momentum of mechanical rotation can be transported into a finite spin, which is known as the Barnett effect. The Barnett effect is an inverse phenomenon of the Einstein-de Haas effect, and these effects are manifestations of the gyromagnetic effects as summarized in Ref. [12]. Then, conversely, it would be a natural anticipation to associate the CVE with a relativistic extension of the Barnett effect. However, there are still some unresolved issues, and so this section must remain speculative.

4.3.1 Chiral Barnett effect

The Barnett effect is quantified by a formula connecting the magnetization, \mathbf{M} , and the angular velocity vector, $\boldsymbol{\omega}$. A quick derivation of the formula is found in Ref. [12], which can be understood in terms of the energy shift. The angular momentum, \mathbf{J} make an energy shift by $\mathbf{J} \cdot \boldsymbol{\omega}$, which is equated to the magnetic energy shift by $\boldsymbol{\mu} \cdot \mathbf{H}_{\text{eff}}$ with the magnetic moment $\boldsymbol{\mu}$ and the effective magnetic field \mathbf{H}_{eff} . The magnetization is $\mathbf{M} = \chi_B \mathbf{H}_{\text{eff}}$ with the magnetic susceptibility and the magnetic moment is $\boldsymbol{\mu} = \gamma \mathbf{J}$ with the gyromagnetic ratio γ . Then, \mathbf{H}_{eff} and $\boldsymbol{\mu}$ can be eliminated, that is, the formula for the Barnett effect obtains as

Barnett Effect: A finite magnetization, \mathbf{M} , along the rotation axis appears for a net charge neutral object spun with the angular velocity $\boldsymbol{\omega}$, which is formulated as

$$\mathbf{M} = \frac{\chi_B}{\gamma} \boldsymbol{\omega} \quad (113)$$

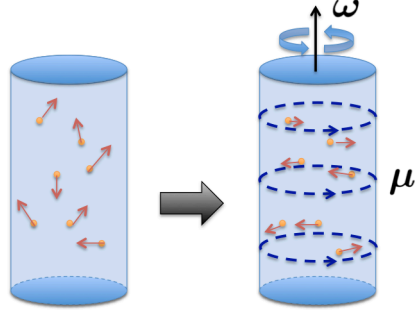


Figure 16: Sketch for the chiral Barnett effect: the spin of chiral fermions is aligned along the momentum direction. For rotating system where fermions collectively have a net momentum on average, the spin expectation value has a transverse component. Figure taken from Ref. [95].

In relativistic generalization the most subtle part is the decomposition of the angular momentum into the orbital and the spin components. What is conserved as a Nöther current is the total angular momentum only, which is immediately found from the Dirac Lagrangian as

$$J^k = \epsilon^{ijk} i\bar{\psi} \left(\gamma^0 x^i \partial^j - \gamma^0 x^j \partial^i + \frac{1}{2} \gamma^0 \gamma^i \gamma^j \right) \psi. \quad (114)$$

It is quite natural, in a sense that the non-relativistic limit is smoothly taken, to consider the first two terms involving the coordinates as the orbital angular momentum and the rest as the spin. Then, this identification leads to $S^k = \frac{1}{2} j_5^k$, that is, the axial vector current itself is the spin. With this hypothetical identification, the spin expectation value is expressed for a given distribution function $f(p)$ as studied in Ref. [95]. The answer up to the first order in the ω expansion and also the \hbar expansion has two contributions:

$$\langle \mathbf{S} \rangle_{R/L} \simeq -\frac{\omega}{2} \int \frac{d^3 p}{(2\pi)^3} f'_{R/L}(p) \mp \frac{\omega \times \mathbf{x}}{6} \int \frac{d^3 p}{(2\pi)^3} p f'_{R/L}(p). \quad (115)$$

This expression uses a little sloppy notation. The subscript R/L denotes a contribution from one-handed fermion sector. The first term is nothing but the CVE current as given in Eq. (94), for which the overall sign \mp in Eq. (94) is absorbed in the definition of $\langle \mathbf{S} \rangle$ identified as the axial vector. This induced spin expectation value yields a finite magnetic moment, so that the longitudinal magnetization is concluded, which is a natural relativistic extension of the conventional Barnett effect.

The physical interpretation of the second term proportional to $\omega \times \mathbf{x}$, which is denoted here by $\langle \mathbf{S} \rangle_{\perp}$, is highly nontrivial. To clarify the intuitive meaning, it would be useful to reexpress it as

$$\langle \mathbf{S} \rangle_{\perp} = \sum_{\pm} \mp \frac{\omega \times \mathbf{x}}{6} \int \frac{d^3 p}{(2\pi)^3} p f'_{R/L}(p) = \frac{\hbar}{2} (\omega \times \mathbf{x}) n_5, \quad (116)$$

where \hbar is recovered to emphasize the physical unit for the angular momentum. Here, we see that $\omega \times \mathbf{x}$ represents the transverse velocity of rotating matter. Because right-handed (left-handed) fermions have the spin alignment in parallel (anti-parallel) to the momentum direction, therefore, this transverse Barnett effect is an inevitable consequence from a combination of chiral imbalance and rotation as graphically shown in Fig. 16. It should be noted that analogous nontrivial effects as results of spin-rotation coupling have been predicted in a different context [96].

4.3.2 Chiral Einstein-de Haas effect

The essence for the Einstein-de Haas effect is the angular momentum conservation. That is, the spin relaxation results in a finite amount of the orbital angular momentum so that the total angular momentum must be conserved. Because the orbital angular momentum is associated with mechanical rotation,

such a transported orbital momentum causes a physical rotation. In this sense, the conservation law is robust, and the relativistic extension should be straightforward.

To concretize the physical setup, let us suppose chiral matter at rest (i.e., no rotation yet). Then, a finite magnetic field is adiabatically introduced into the system. A finite spin expectation value grows up in response to imposed magnetic field. Actually, the magnetic field itself applied to charged particles carries a finite angular momentum as argued in Ref. [97], which makes the realization of conservation law a little complicated. Once the spin operator in relativistic theory is identified as the axial vector current, it is a classically conserved quantity for chiral matter with $m = 0$. This means that, without \mathcal{P} - and \mathcal{CP} -violating electromagnetic background, therefore, the integrated spin averaged over the whole system should be vanishing, and so the angular momentum of the magnetic field cannot be received by the spin but may be maximally transferred to the orbital angular momentum only, leading to an enhancement in the Einstein-de Haas effect. This conjecture still awaits to be formulated and quantified by field-theoretical investigations.

5 Summary

As excused in the beginning, this review is not a summarizing report to cover all related works with balanced weights, but it is more like a story along a history of my own research interest. The order of sections, subsections, subsubsections, therefore, has inevitability for me as if the order of historical events had definite inevitability. I must apologize for not mentioning all relevant works, which is in any case impossible.

In this review I tried to spell out calculation procedures especially in the early sections, so that readers can reproduce the main results, and if necessary, can make use of the method for further applications. For practical purposes Schwinger's proper-time integral is the most convenient approach, but I preferred to start with explicit solutions of the free Dirac equation. This is because the complete set of wave-functions contains more detailed information than the propagator. For example, to take account of finite size effect, the most straightforward strategy is to solve the Dirac equation under an imposed boundary condition. Also, for problems with finite rotation, this rather brute-force method is useful for clarity.

The magnetic catalysis is the most important phenomenon of chiral matter put in magnetic field. Because there are already very nice review articles to explicate what it is, I tried to give only minimal direct calculations within a range reproducible for readers. In this part I gave rather detailed explanations in terms of the renormalization group. The physical contents are equivalent to direct calculations but such an intuitive view to understand physics is quite interesting. Actually, I learnt this RG argument from Jan Pawłowski who is an expert on the functional RG approach, and then I felt like that my eyes were reopened to a new streak of light. I hope that some readers may find this RG argument inspiring as I once did.

Nowadays, it is impossible to skip discussion on the inverse magnetic catalysis once the magnetic catalysis is concerned. This is a puzzle noticed in the research field of the strong interaction, and some people tend to think that this puzzle has been already settled down, but some other people are not yet satisfied. In this review I tried to make it understandable why and in what context the inverse magnetic catalysis was so shocking and perplexing.

Everybody would agree that the inclusion of electric field is the next step after treating situations with magnetic field alone. The problem, however, becomes far more difficult by orders of magnitude. This is so because the problem cannot be static any longer but should be dynamical as soon as the external electric field is involved, which can be alternatively understood as the sign problem in numerical Monte-Carlo simulations. Thus, phase diagrams with an axis of external magnetic field can exist, while matter exposed to external electric field cannot be classified into equilibrated distinct phases.

A new element brought in by electric field is the particle production from quantum fluctuations. In a sense the vacuum in quantum field theory should be not an empty state but more like a medium, and the particle production from the vacuum, known as the Schwinger Mechanism, is a phenomenon of insulator-metal transition in solid state physics. In the presence of both electric and magnetic fields, interestingly, such background fields break \mathcal{P} - and \mathcal{CP} -symmetries, and the particle-anti-particle symmetry is violated then. This violation causes an unbalanced distribution of chirality, that is, a finite difference between right-handed and left-handed particles. This kind of chiral unbalanced matter under magnetic field is an ideal device to realize the chiral magnetic effect. Regarding the physical interpretation, since when Dmitri Kharzeev, Harmen Warringa, and I published a paper on the CME, it had been a puzzle how to distinguish the genuine current in real time and the Euclidean and thus static expectation value of the current operator. For example, in lattice discretized numerical simulation, it is always possible to measure the current operator expectation value, but such Euclidean formulation cannot be a proper description of real-time phenomena. After 10 years since our paper on the CME, I believe that, thanks to collaboration with Patrick Copinger and Shi Pu, I eventually reached a clear way to understand the difference between the Minkowskian and the Euclidean quantities using the in- and out-states. I would emphasize that using the chiral chemical potential, μ_5 , is a very convenient bookkeeping device, but, if controversies are fomented by μ_5 , an alternative and more physical formulation with $\mathbf{E} \cdot \mathbf{B}$ would be helpful to resolve confusions.

Analogy between the magnetic field and the rotation is another longstanding problem. I learnt a lot about the Floquet theory from Takashi Oka to know that the Floquet engineering is such a promising technique to test various ideas of relativistic quantum field theory such as the quantum anomaly. With this technique, even theory fictions like axial vector potentials can be implemented in real experiments. Now, the applications of synthetic magnetic field (aka, artificial gauge potential) have been a wide spreading subject, and it is not a radical idea at all to expect some Floquet engineering suited for studies on the CME and the analogous phenomenon, i.e., the chiral vortical effect.

The last part of this review is about some ongoing research on the relativistic generalization of classic themes, namely, the Barnett effect and the Einstein-de Haas effect. Usually the Barnett effect is proportional to the mass (since the gyromagnetic ratio γ is inversely proportional to the mass), heavier particles like nuclei would be more desirable than lighter particles like electrons for experimental observation. However, at the same time, the spin-orbit coupling is a relativistic effect, and it should be enhanced for chiral fermions. Then, it is a highly nontrivial question whether such gyromagnetic effects are enhanced or suppressed when the physical system transits from the non-relativistic to the ultra-relativistic limit. This part still awaits further theoretical and experimental investigations.

Acknowledgments

The author thanks Hao-Lei Chen, Patrick Copinger, Shu Ebiyara, Antonino Flachi, Francois Gelis, Yoshimasa Hidaka, Xu-Guang Huang, Dmitri Kharzeev, Tuomas Lappi, Kazuya Mameda, Takashi Oka, Jan Pawłowski, Shi Pu, Zebin Qiu, Harmen Warringa for discussions and collaborations. The author learnt a lot from collaborations with them, and this review is based on papers coauthored with them. This work was supported by JSPS KAKENHI Grant No. 18H01211.

References

- [1] D. Lai, “Matter in strong magnetic fields,” *Rev. Mod. Phys.* **73** (2001) 629–662.

- [2] V. A. Miransky and I. A. Shovkovy, “Quantum field theory in a magnetic field: From quantum chromodynamics to graphene and Dirac semimetals,” *Phys. Rept.* **576** (2015) 1–209, [arXiv:1503.00732 \[hep-ph\]](#).
- [3] K. Hattori and X.-G. Huang, “Novel quantum phenomena induced by strong magnetic fields in heavy-ion collisions,” *Nucl. Sci. Tech.* **28** (2017) 26, [arXiv:1609.00747 \[nucl-th\]](#).
- [4] D. E. Kharzeev, J. Liao, S. A. Voloshin, and G. Wang, “Chiral magnetic and vortical effects in high-energy nuclear collisions-A status report,” *Prog. Part. Nucl. Phys.* **88** (2016) 1–28, [arXiv:1511.04050 \[hep-ph\]](#).
- [5] G. V. Dunne, “Heisenberg-Euler effective Lagrangians: Basics and extensions,” in *From fields to strings: Circumnavigating theoretical physics. Ian Kogan memorial collection (3 volume set)*, M. Shifman, A. Vainshtein, and J. Wheeler, eds., pp. 445–522. 2004. [arXiv:hep-th/0406216 \[hep-th\]](#).
- [6] F. Gelis and N. Tanji, “Schwinger mechanism revisited,” *Prog. Part. Nucl. Phys.* **87** (2016) 1–49, [arXiv:1510.05451 \[hep-ph\]](#).
- [7] K. Fukushima, “Views of the chiral magnetic effect,” *Lect. Notes Phys.* **871** (2013) 241–259, [arXiv:1209.5064 \[hep-ph\]](#).
- [8] P.-G. de Gennes, *Superconductivity of Metals and Alloys*. Advanced book classics. Advanced Book Program, Perseus Books, 1999.
- [9] W. Domcke, P. Hänggi, and D. Tannor, “Driven Quantum Systems,” *Special Issue : Chem. Phys.* **217** (1997) 117–416.
- [10] M. Bukov, L. D’Alessio, and A. Polkovnikov, “Universal high-frequency behavior of periodically driven systems: from dynamical stabilization to floquet engineering,” *Advances in Physics* **64** (2015) 139–226.
- [11] J. Dalibard, F. Gerbier, G. Juzeliūnas, and P. Öhberg, “Colloquium: Artificial gauge potentials for neutral atoms,” *Rev. Mod. Phys.* **83** (2011) 1523–1543.
- [12] S. J. Barnett, “Gyromagnetic and electron-inertia effects,” *Rev. Mod. Phys.* **7** (1935) 129–166.
- [13] V. Ritus, “Radiative corrections in quantum electrodynamics with intense field and their analytical properties,” *Annals of Physics* **69** (1972) 555 – 582.
- [14] J. S. Schwinger, “On gauge invariance and vacuum polarization,” *Phys. Rev.* **82** (1951) 664–679.
- [15] V. P. Gusynin, V. A. Miransky, and I. A. Shovkovy, “Dimensional reduction and dynamical chiral symmetry breaking by a magnetic field in (3+1)-dimensions,” *Phys. Lett.* **B349** (1995) 477–483, [arXiv:hep-ph/9412257 \[hep-ph\]](#).
- [16] V. P. Gusynin, V. A. Miransky, and I. A. Shovkovy, “Dimensional reduction and catalysis of dynamical symmetry breaking by a magnetic field,” *Nucl. Phys.* **B462** (1996) 249–290, [arXiv:hep-ph/9509320 \[hep-ph\]](#).
- [17] K. Fukushima and Y. Hidaka, “Magnetic catalysis versus magnetic inhibition,” *Phys. Rev. Lett.* **110** (2013) 031601, [arXiv:1209.1319 \[hep-ph\]](#).
- [18] H. Suganuma and T. Tatsumi, “On the behavior of symmetry and phase transitions in a strong electromagnetic field,” *Annals Phys.* **208** (1991) 470–508.

- [19] I. A. Shushpanov and A. V. Smilga, “Quark condensate in a magnetic field,” *Phys. Lett.* **B402** (1997) 351–358, [arXiv:hep-ph/9703201 \[hep-ph\]](#).
- [20] T. D. Cohen, D. A. McGady, and E. S. Werbos, “The Chiral condensate in a constant electromagnetic field,” *Phys. Rev.* **C76** (2007) 055201, [arXiv:0706.3208 \[hep-ph\]](#).
- [21] V. P. Gusynin, V. A. Miransky, and I. A. Shovkovy, “Catalysis of dynamical flavor symmetry breaking by a magnetic field in (2+1)-dimensions,” *Phys. Rev. Lett.* **73** (1994) 3499–3502, [arXiv:hep-ph/9405262 \[hep-ph\]](#). [Erratum: *Phys. Rev. Lett.* 76,1005(1996)].
- [22] S. P. Klevansky, “The Nambu-Jona-Lasinio model of quantum chromodynamics,” *Rev. Mod. Phys.* **64** (1992) 649–708.
- [23] T. Hatsuda and T. Kunihiro, “QCD phenomenology based on a chiral effective Lagrangian,” *Phys. Rept.* **247** (1994) 221–367, [arXiv:hep-ph/9401310 \[hep-ph\]](#).
- [24] D. D. Scherer and H. Gies, “Renormalization group study of magnetic catalysis in the 3d Gross-Neveu model,” *Phys. Rev.* **B85** (2012) 195417, [arXiv:1201.3746 \[cond-mat.str-el\]](#).
- [25] K. Fukushima and J. M. Pawłowski, “Magnetic catalysis in hot and dense quark matter and quantum fluctuations,” *Phys. Rev.* **D86** (2012) 076013, [arXiv:1203.4330 \[hep-ph\]](#).
- [26] F. Preis, A. Rebhan, and A. Schmitt, “Inverse magnetic catalysis in dense holographic matter,” *JHEP* **03** (2011) 033, [arXiv:1012.4785 \[hep-th\]](#).
- [27] F. Preis, A. Rebhan, and A. Schmitt, “Inverse magnetic catalysis in field theory and gauge-gravity duality,” *Lect. Notes Phys.* **871** (2013) 51–86, [arXiv:1208.0536 \[hep-ph\]](#).
- [28] G. S. Bali, F. Bruckmann, G. Endrodi, Z. Fodor, S. D. Katz, S. Krieg, A. Schafer, and K. K. Szabo, “The QCD phase diagram for external magnetic fields,” *JHEP* **02** (2012) 044, [arXiv:1111.4956 \[hep-lat\]](#).
- [29] K. Fukushima, “Chiral effective model with the Polyakov loop,” *Phys. Lett.* **B591** (2004) 277–284, [arXiv:hep-ph/0310121 \[hep-ph\]](#).
- [30] C. Ratti, M. A. Thaler, and W. Weise, “Phases of QCD: Lattice thermodynamics and a field theoretical model,” *Phys. Rev.* **D73** (2006) 014019, [arXiv:hep-ph/0506234 \[hep-ph\]](#).
- [31] A. J. Mizher, M. N. Chernodub, and E. S. Fraga, “Phase diagram of hot QCD in an external magnetic field: possible splitting of deconfinement and chiral transitions,” *Phys. Rev.* **D82** (2010) 105016, [arXiv:1004.2712 \[hep-ph\]](#).
- [32] R. Gatto and M. Ruggieri, “Quark Matter in a Strong Magnetic Background,” *Lect. Notes Phys.* **871** (2013) 87–119, [arXiv:1207.3190 \[hep-ph\]](#).
- [33] G. S. Bali, F. Bruckmann, G. Endrodi, Z. Fodor, S. D. Katz, and A. Schafer, “QCD quark condensate in external magnetic fields,” *Phys. Rev.* **D86** (2012) 071502, [arXiv:1206.4205 \[hep-lat\]](#).
- [34] G. S. Bali, F. Bruckmann, G. Endrodi, F. Gruber, and A. Schaefer, “Magnetic field-induced gluonic (inverse) catalysis and pressure (an)isotropy in QCD,” *JHEP* **04** (2013) 130, [arXiv:1303.1328 \[hep-lat\]](#).
- [35] K. Fukushima, “Magnetic-field induced screening effect and collective excitations,” *Phys. Rev.* **D83** (2011) 111501, [arXiv:1103.4430 \[hep-ph\]](#).

- [36] K. Hattori and K. Itakura, “Vacuum birefringence in strong magnetic fields: (I) Photon polarization tensor with all the Landau levels,” *Annals Phys.* **330** (2013) 23–54, [arXiv:1209.2663 \[hep-ph\]](#).
- [37] K. Hattori and K. Itakura, “Vacuum birefringence in strong magnetic fields: (II) Complex refractive index from the lowest Landau level,” *Annals Phys.* **334** (2013) 58–82, [arXiv:1212.1897 \[hep-ph\]](#).
- [38] F. Bruckmann, G. Endrodi, and T. G. Kovacs, “Inverse magnetic catalysis and the Polyakov loop,” *JHEP* **04** (2013) 112, [arXiv:1303.3972 \[hep-lat\]](#).
- [39] E. J. Ferrer, V. de la Incera, and X. J. Wen, “Quark Antiscreening at Strong Magnetic Field and Inverse Magnetic Catalysis,” *Phys. Rev.* **D91** (2015) no. 5, 054006, [arXiv:1407.3503 \[nucl-th\]](#).
- [40] N. Mueller and J. M. Pawłowski, “Magnetic catalysis and inverse magnetic catalysis in QCD,” *Phys. Rev.* **D91** (2015) 116010, [arXiv:1502.08011 \[hep-ph\]](#).
- [41] G. Endrödi, “QCD equation of state at nonzero magnetic fields in the Hadron Resonance Gas model,” *JHEP* **04** (2013) 023, [arXiv:1301.1307 \[hep-ph\]](#).
- [42] K. Fukushima and Y. Hidaka, “Magnetic shift of the chemical freeze-out and electric charge fluctuations,” *Phys. Rev. Lett.* **117** (2016) no. 10, 102301, [arXiv:1605.01912 \[hep-ph\]](#).
- [43] D. Cangemi, E. D’Hoker, and G. V. Dunne, “Effective energy for QED in (2+1)-dimensions with semilocalized magnetic fields: A Solvable model,” *Phys. Rev.* **D52** (1995) R3163–R3167, [arXiv:hep-th/9506085 \[hep-th\]](#).
- [44] Y. Aharonov and A. Casher, “Ground state of a spin-1/2 charged particle in a two-dimensional magnetic field,” *Phys. Rev. A* **19** (1979) 2461–2462.
- [45] P. Copinger and K. Fukushima, “Spatially assisted Schwinger Mechanism and magnetic catalysis,” *Phys. Rev. Lett.* **117** (2016) 081603, [arXiv:1605.05957 \[hep-th\]](#). [Erratum: *Phys. Rev. Lett.* 118, no. 9, 099903 (2017)].
- [46] H.-L. Chen, K. Fukushima, X.-G. Huang, and K. Mameda, “Surface magnetic catalysis,” *Phys. Rev.* **D96** (2017) 054032, [arXiv:1707.09130 \[hep-ph\]](#).
- [47] J. Schwinger, “On gauge invariance and vacuum polarization,” *Phys. Rev.* **82** (1951) 664–679.
- [48] T. D. Cohen and D. A. McGady, “The Schwinger mechanism revisited,” *Phys. Rev.* **D78** (2008) 036008, [arXiv:0807.1117 \[hep-ph\]](#).
- [49] K. Fukushima, F. Gelis, and T. Lappi, “Multiparticle correlations in the Schwinger mechanism,” *Nucl. Phys.* **A831** (2009) 184–214, [arXiv:0907.4793 \[hep-ph\]](#).
- [50] G. ’t Hooft, “The Scattering matrix approach for the quantum black hole: An Overview,” *Int. J. Mod. Phys.* **A11** (1996) 4623–4688, [arXiv:gr-qc/9607022 \[gr-qc\]](#).
- [51] A. I. Nikishov, “Barrier scattering in field theory removal of klein paradox,” *Nucl. Phys.* **B21** (1970) 346–358.
- [52] N. Tanji, “Dynamical view of pair creation in uniform electric and magnetic fields,” *Annals Phys.* **324** (2009) 1691–1736, [arXiv:0810.4429 \[hep-ph\]](#).

- [53] C. Schubert, “Perturbative quantum field theory in the string inspired formalism,” *Phys. Rept.* **355** (2001) 73–234, [arXiv:hep-th/0101036 \[hep-th\]](#).
- [54] R. Schutzhold, H. Gies, and G. Dunne, “Dynamically assisted Schwinger mechanism,” *Phys. Rev. Lett.* **101** (2008) 130404, [arXiv:0807.0754 \[hep-th\]](#).
- [55] H. B. Nielsen and M. Ninomiya, “Adler-Bell-Jackiw anomaly and Weyl fermions in crystal,” *Phys. Lett.* **130B** (1983) 389–396.
- [56] E. Fradkin, D. Guitman, and S. Shvartsman, *Quantum electrodynamics: with unstable vacuum*. Springer series in nuclear and particle physics. Springer-Verlag, 1991.
- [57] P. Copinger, K. Fukushima, and S. Pu, “Axial Ward identity and the Schwinger mechanism – Applications to the real-time chiral magnetic effect and condensates,” [arXiv:1807.04416 \[hep-th\]](#).
- [58] H. J. Warringa, “Dynamics of the Chiral Magnetic Effect in a weak magnetic field,” *Phys. Rev.* **D86** (2012) 085029, [arXiv:1205.5679 \[hep-th\]](#).
- [59] F. Wilczek, “Two applications of axion electrodynamics,” *Phys. Rev. Lett.* **58** (1987) 1799.
- [60] K. Fukushima, D. E. Kharzeev, and H. J. Warringa, “The Chiral Magnetic Effect,” *Phys. Rev.* **D78** (2008) 074033, [arXiv:0808.3382 \[hep-ph\]](#).
- [61] A. Vilenkin, “Equilibrium parity violating current in a magnetic field,” *Phys. Rev.* **D22** (1980) 3080–3084.
- [62] M. Giovannini and M. Shaposhnikov, “Primordial magnetic fields, anomalous isocurvature fluctuations and big bang nucleosynthesis,” *Phys. Rev. Lett.* **80** (1998) 22–25, [arXiv:hep-ph/9708303 \[hep-ph\]](#).
- [63] M. M. Vazifeh and M. Franz, “Electromagnetic response of weyl semimetals,” *Phys. Rev. Lett.* **111** (2013) 027201.
- [64] N. Yamamoto, “Generalized Bloch theorem and chiral transport phenomena,” *Phys. Rev.* **D92** (2015) no. 8, 085011, [arXiv:1502.01547 \[cond-mat.mes-hall\]](#).
- [65] K. Fukushima, D. E. Kharzeev, and H. J. Warringa, “Real-time dynamics of the Chiral Magnetic Effect,” *Phys. Rev. Lett.* **104** (2010) 212001, [arXiv:1002.2495 \[hep-ph\]](#).
- [66] D. T. Son and B. Z. Spivak, “Chiral anomaly and classical negative magnetoresistance of Weyl metals,” *Phys. Rev.* **B88** (2013) 104412, [arXiv:1206.1627 \[cond-mat.mes-hall\]](#).
- [67] Q. Li, D. E. Kharzeev, C. Zhang, Y. Huang, I. Pletikosic, A. V. Fedorov, R. D. Zhong, J. A. Schneeloch, G. D. Gu, and T. Valla, “Observation of the chiral magnetic effect in ZrTe5,” *Nature Phys.* **12** (2016) 550–554, [arXiv:1412.6543 \[cond-mat.str-el\]](#).
- [68] K. Fukushima and Y. Hidaka, “Electric conductivity of hot and dense quark matter in a magnetic field with Landau level resummation via kinetic equations,” *Phys. Rev. Lett.* **120** (2018) no. 16, 162301, [arXiv:1711.01472 \[hep-ph\]](#).
- [69] Y. Jiang and J. Liao, “Pairing phase transitions of matter under rotation,” *Phys. Rev. Lett.* **117** (2016) no. 19, 192302, [arXiv:1606.03808 \[hep-ph\]](#).

- [70] M. N. Chernodub and S. Gongyo, “Effects of rotation and boundaries on chiral symmetry breaking of relativistic fermions,” *Phys. Rev.* **D95** (2017) no. 9, 096006, [arXiv:1702.08266 \[hep-th\]](#).
- [71] Y. Liu and I. Zahed, “Pion condensation by rotation in a magnetic field,” *Phys. Rev. Lett.* **120** (2018) no. 3, 032001, [arXiv:1711.08354 \[hep-ph\]](#).
- [72] H.-L. Chen, K. Fukushima, X.-G. Huang, and K. Mameda, “Analogy between rotation and density for Dirac fermions in a magnetic field,” *Phys. Rev.* **D93** (2016) no. 10, 104052, [arXiv:1512.08974 \[hep-ph\]](#).
- [73] F. Becattini and L. Tinti, “The Ideal relativistic rotating gas as a perfect fluid with spin,” *Annals Phys.* **325** (2010) 1566–1594, [arXiv:0911.0864 \[gr-qc\]](#).
- [74] A. Vilenkin, “Parity violating currents in thermal radiation,” *Phys. Lett.* **80B** (1978) 150–152.
- [75] A. Vilenkin, “Macroscopic parity violating effects: neutrino fluxes from rotating black holes and in rotating thermal radiation,” *Phys. Rev.* **D20** (1979) 1807–1812.
- [76] A. Vilenkin, “Quantum field theory at finite temperature in a rotating system,” *Phys. Rev.* **D21** (1980) 2260–2269.
- [77] K. Landsteiner, E. Megias, and F. Pena-Benitez, “Gravitational anomaly and transport,” *Phys. Rev. Lett.* **107** (2011) 021601, [arXiv:1103.5006 \[hep-ph\]](#).
- [78] K. Landsteiner, E. Megias, L. Melgar, and F. Pena-Benitez, “Holographic gravitational anomaly and chiral vortical effect,” *JHEP* **09** (2011) 121, [arXiv:1107.0368 \[hep-th\]](#).
- [79] K. Jensen, R. Loganayagam, and A. Yarom, “Thermodynamics, gravitational anomalies and cones,” *JHEP* **02** (2013) 088, [arXiv:1207.5824 \[hep-th\]](#).
- [80] K. Jensen, R. Loganayagam, and A. Yarom, “Anomaly inflow and thermal equilibrium,” *JHEP* **05** (2014) 134, [arXiv:1310.7024 \[hep-th\]](#).
- [81] S. Golkar and D. T. Son, “(Non)-renormalization of the chiral vortical effect coefficient,” *JHEP* **02** (2015) 169, [arXiv:1207.5806 \[hep-th\]](#).
- [82] S. Golkar and S. Sethi, “Global anomalies and effective field theory,” *JHEP* **05** (2016) 105, [arXiv:1512.02607 \[hep-th\]](#).
- [83] D. T. Son and P. Surowka, “Hydrodynamics with triangle anomalies,” *Phys. Rev. Lett.* **103** (2009) 191601, [arXiv:0906.5044 \[hep-th\]](#).
- [84] M. Buzzegoli, E. Grossi, and F. Becattini, “General equilibrium second-order hydrodynamic coefficients for free quantum fields,” *JHEP* **10** (2017) 091, [arXiv:1704.02808 \[hep-th\]](#). [Erratum: JHEP07,119(2018)].
- [85] A. Flachi and K. Fukushima, “Chiral vortical effect with finite rotation, temperature, and curvature,” *Phys. Rev.* **D98** (2018) no. 9, 096011, [arXiv:1702.04753 \[hep-th\]](#).
- [86] A. Flachi and K. Fukushima, “Chiral mass-gap in curved space,” *Phys. Rev. Lett.* **113** (2014) no. 9, 091102, [arXiv:1406.6548 \[hep-th\]](#).
- [87] M. N. Chernodub, A. Cortijo, and K. Landsteiner, “Zilch vortical effect,” *Phys. Rev.* **D98** (2018) no. 6, 065016, [arXiv:1807.10705 \[hep-th\]](#).

- [88] T. Mori, T. Kuwahara, and K. Saito, “Rigorous bound on energy absorption and generic relaxation in periodically driven quantum systems,” *Phys. Rev. Lett.* **116** (2016) 120401.
- [89] S. Blanes, F. Casas, J. Oteo, and J. Ros, “The magnus expansion and some of its applications,” *Physics Reports* **470** (2009) no. 5, 151 – 238.
- [90] S. Ebihara, K. Fukushima, and T. Oka, “Chiral pumping effect induced by rotating electric fields,” *Phys. Rev.* **B93** (2016) no. 15, 155107, [arXiv:1509.03673 \[cond-mat.str-el\]](#).
- [91] S. Ebihara, K. Fukushima, and K. Mameda, “Boundary effects and gapped dispersion in rotating fermionic matter,” *Phys. Lett.* **B764** (2017) 94–99, [arXiv:1608.00336 \[hep-ph\]](#).
- [92] K. Hattori and Y. Yin, “Charge redistribution from anomalous magnetovorticity coupling,” *Phys. Rev. Lett.* **117** (2016) no. 15, 152002, [arXiv:1607.01513 \[hep-th\]](#).
- [93] T. Oka and S. Kitamura, “Floquet engineering of quantum materials,” *Annual Review of Condensed Matter Physics* **10** (2019) no. 1, 387–408.
- [94] H. Sambe, “Steady states and quasienergies of a quantum-mechanical system in an oscillating field,” *Phys. Rev. A* **7** (1973) 2203–2213.
- [95] K. Fukushima, S. Pu, and Z. Qiu, “Eddy magnetization from the chiral Barnett effect,” [arXiv:1808.08016 \[hep-ph\]](#).
- [96] M. Matsuo, J. Ieda, E. Saitoh, and S. Maekawa, “Effects of mechanical rotation on spin currents,” *Phys. Rev. Lett.* **106** (2011) 076601.
- [97] C. R. Greenshields, R. L. Stamps, S. Franke-Arnold, and S. M. Barnett, “Is the angular momentum of an electron conserved in a uniform magnetic field?,” *Phys. Rev. Lett.* **113** (2014) 240404.